

GAIN AND OFFSET ERROR CORRECTION FOR CMOS IMAGE SENSOR USING
DELTA-SIGMA MODULATION

by

Kuang Ming Yap

A thesis

submitted in partial fulfillment

of the requirements for the degree of

Master of Science in Electrical Engineering

Boise State University

May 2010

BOISE STATE UNIVERSITY GRADUATE COLLEGE

DEFENSE COMMITTEE AND FINAL READING APPROVALS

of the thesis submitted by

Kuang Ming Yap

Thesis Title: Gain and Offset Error Correction for CMOS Image Sensor Using Delta-Sigma Modulation

Date of Final Oral Examination: 26 March 2010

The following individuals read and discussed the thesis submitted by student Kuang Ming Yap, and they also evaluated his presentation and response to questions during the final oral examination. They found that the student passed the final oral examination, and that the thesis was satisfactory for a master's degree and ready for any final modifications that they explicitly required.

R. Jacob Baker, Ph.D. Chair, Supervisory Committee

Maria Mitkova, Ph.D. Member, Supervisory Committee

Jennifer A. Smith, Ph.D. Member, Supervisory Committee

The final reading approval of the thesis was granted by R. Jacob Baker, Ph.D., Chair of the Supervisory Committee. The thesis was approved for the Graduate College by John R. Pelton, Ph.D., Dean of the Graduate College.

ACKNOWLEDGEMENTS

I would like to express my sincere gratitude to my advisor, Dr. Jake Baker, for his encouragement, guidance, and support during my student years here at Boise State University. His motivation and determination to help all of his students has been inspirational. He has been most helpful during my thesis. He was willing to meet me during late evenings and weekends if I had trouble with my thesis.

I also would like to thank Dr. Maria Mitkova and Dr. Jennifer Smith for their time and effort as committee members for my thesis defense. Last but not least, I would also like to thank my wife, Sue-Fern, for her love and support during my years as a Master student.

ABSTRACT

A delta-sigma modulation analog-to-digital converter (ADC) has many benefits over the use of a pipeline ADC in a CMOS image sensor. These benefits include lower power, noise reduction, ease of maximizing the input range, and simpler signal routing for large arrays. Multiple delta-sigma modulation ADCs are required in a CMOS image sensor, one for each pixel column. Any voltage threshold mismatch between ADCs will introduce gain and offset errors in the ADC's transfer function. These errors will lead to fixed-pattern noise. Correcting gain and offset error for every ADCs in the image sensor will require a complex digital signal processor. This thesis presents techniques to minimize the effects of gain and offset errors in delta-sigma modulation ADCs for CMOS image sensors.

TABLE OF CONTENTS

ACKNOWLEDGMENTS.....	iii
ABSTRACT.....	iv
LIST OF TABLES.....	vii
LIST OF FIGURES.....	viii
LIST OF ABBREVIATIONS.....	xi
CHAPTER 1: INTRODUCTION.....	1
1.1 Motivation.....	1
1.2 Thesis Contribution.....	2
1.3 Various CMOS Pixel Architectures.....	3
1.3.1 The Passive Pixel.....	4
1.3.2 PIN Photodiode-Type APS.....	8
1.3.3 Pinned Photodiode-Type APS.....	12
1.3.4 Photogate-Type APS.....	16
1.3.5 Logarithmic APS.....	17
1.4 An Overview of the Use of Correlated Double Sampling in an APS.....	19
CHAPTER 2: CMOS IMAGE SENSOR USING DELTA-SIGMA ADC.....	23
2.1 An Analogy for the Delta-Sigma Modulator.....	23
2.2 Sensing Scheme for a DSM in a CMOS Image Sensor.....	24

2.3 DSM Operation in a CMOS Image Sensor.....	26
2.4 CMOS Image Sensor DSM with Reference Path.....	37
2.5 CMOS Image Sensor DSM with Reference Path and Input Path Switching	43
2.6 CMOS Image Sensor DSM with Reference Path, Input Path Switching and Gain Error Correction.....	48
CHAPTER 3: SIMULATION RESULTS AND TEST CHIP INFORMATION.....	57
3.1 Simulation Results.....	57
3.2 Layout.....	62
3.3 General Test Chip Information.....	63
CHAPTER 4: CONCLUSION AND FUTURE WORK.....	65
4.1 Conclusion.....	65
4.2 Future Work.....	66
REFERENCES.....	67

LIST OF TABLES

Table 3.5 Pin Description.....	64
--------------------------------	----

LIST OF FIGURES

Figure 1.1 Diagram showing that the charge stored on the photodiode is being neutralized when it is exposed to light.....	4
Figure 1.2 A schematic diagram for a CMOS passive pixel [3].....	5
Figure 1.3 A layout diagram of an 8x8 pixel array.....	6
Figure 1.4 A schematic diagram for a passive pixel CMOS imager with a charge integrating amplifier [4].....	7
Figure 1.5 Schematic diagram for the photodiode-type APS [3].....	8
Figure 1.6 A cross-section image of a PIN photodiode.....	10
Figure 1.7 A SCM cross-section profile of the photo-cathodes in the Foveon F018-50-F19A.....	11
Figure 1.8 A diagram of a pinned-photodiode pixel sensor [3].....	13
Figure 1.9 An image of a pinned-photodiode.....	14
Figure 1.10 A diagram showing the output of a CDS is free of noise and voltage mismatches.....	15
Figure 1.11 Schematic diagram of a photogate APS [3].....	17
Figure 1.12 Schematic Diagram of a standard logarithmic APS [3].....	18
Figure 1.13 Schematic used to illustrate correlated double sampling.....	20
Figure 2.1 A picture that demonstrates the general idea of a DSM ADC.....	23

Figure 2.2 A 4x4 pixel diagram of a DSM CMOS Imager.....	25
Figure 2.3 Schematic of a Basic CMOS Imager Delta Sigma Modulator [2].....	28
Figure 2.4 Schematic to determine the optimum source-follower transistor size.....	29
Figure 2.5 A DC sweep on the five PMOS source follower-transistor in Figure 2.4 with its source terminal as the output.....	29
Figure 2.6 The slope of the source terminal (output) for the DC sweep simulation on the five PMOS source-follower transistors in Figure 2.4.....	30
Figure 2.7 A simulation schematic used to compare body-effect in PMOS source-followers.....	32
Figure 2.8 The differentiated output source voltage signal used to compare body- effect in PMOS source-followers.....	33
Figure 2.9 The waveform of a 2-phase non-overlapping clock.....	34
Figure 2.10 Basic CMOS Imager DSM Input-Output Transfer Function.....	37
Figure 2.11 Schematic of a CMOS Imager Delta Sigma Modulator with reference Path [2].....	38
Figure 2.12 CMOS Imager DSM with Reference Path Input-Output Transfer Function.....	41
Figure 2.13 Comparing the ideal transfer function of a Reference Path CMOS Imager DSM to a transfer function with different threshold voltage mismatches.....	42
Figure 2.14 Schematic of a CMOS Imager Delta Sigma Modulator with reference path and input path switching [1].....	44
Figure 2.15 Schematic of a CMOS Imager Delta Sigma Modulator with gain error correction.....	49

Figure 2.16 Schematic diagram of a 4-phase non-overlapping clock generator.....	50
Figure 2.17 The waveform of a 4-phase non-overlapping clock signal. The bottom figure shows the close-up view when transitioning from the first phase to the second phase.....	50
Figure 2.18 Schematic of a CMOS Imager Delta Sigma Modulator with reference path, input path switching, and gain error correction.....	54
Figure 3.1 Simulation Results for the CMOS Imager DSM with reference path. Different voltage offsets were applied to the gate of M12 and M5 to simulate offset and gain error.....	58
Figure 3.2 Simulation Results for the CMOS Imager DSM with reference path and gain error correction. Different voltage offsets were applied to the gate of M12 and M5 to simulate offset and gain error.....	59
Figure 3.3 Simulation Results for the CMOS Imager DSM with reference path, input path switching, and gain error correction. A 0.25V voltage offsets was applied to the gate of M5 to simulate offset error.....	60
Figure 3.4 Simulation Results for the CMOS Imager DSM with reference path, input path switching, and gain error correction. Different voltages offsets were applied to M5 and M12 to simulate offset and gain error.....	61
Figure 3.5 Test chip full layout.....	62
Figure 3.6 Bonding diagram for test chip provided by MOSIS.....	63

LIST OF ABBREVIATIONS

ADC	Analog-to-Digital Converter
APS	Active Pixel Sensor
CDS	Correlated Double Sampling
CMOS	Complementary Metal-Oxide Semiconductor
DAC	Digital-to-Analog Converter
DSM	Delta-Sigma Modulator
FPN	Fixed-Pattern Noise
SCM	Scanning Capacitance Microscopy

CHAPTER 1: INTRODUCTION

1.1 Motivation

The pipeline analog-to-digital converter (ADC) is currently used in today's complementary metal-oxide semiconductor (CMOS) image sensors to convert the analog pixel integration voltage to a digital code. There is one pipeline ADC in a CMOS image sensor that detects the color on each color pixel in the array: green, blue, and red [1]. As the density of the CMOS image sensor increases, or the level of color quality increases, the pipeline ADC will require a larger layout area and consume more power. Furthermore, as the size and density of the CMOS image sensor increases, coupled noise and voltage variations, resulting from the long distance required to route the signal between the pixel and the pipeline ADC, become an issue.

One potential solution to these problems is to use a per column delta-sigma modulation (DSM) sensing circuit [1]. The DSM can be introduced to help reduce the large layout area, power and routing issues associated with using a pipeline ADC [2]. The simplest design uses a DSM ADC for each column. This means that if there are 7680 pixel columns in an image sensor, there will be 7680 DSM ADCs on the bottom of the array. Therefore, each of the DSM ADC's input/output curves needs to be identical.

However, most of the time, the transfer function of each DSM ADC will not be similar due to transistor voltage-threshold variations that lead to mismatches. This voltage-threshold variation increases as the process technology shrinks. The mismatches lead to fixed-pattern noise and the need for a complex digital-signal processor to compensate for the errors introduced by each DSM ADC. As an example, if there are 7680 DSM ADCs, the digital-signal processor will have to calibrate and compensate for the errors for each of the 7680 DSM ADCs. CMOS imagers using a single pipeline ADC do not suffer from this drawback because of the common signal path each pixel sees. Unfortunately, the drawback of using the pipeline ADC is that it has to operate very quickly to process the large amount of data generated during each row time.

This thesis discusses some of the variations and mismatches found in the DSM ADC that may cause fixed-pattern noise. The thesis also presents some techniques used to help reduce the effects of these variations. With the reduction of fixed-pattern noise, limited by the pixel mismatches themselves, a less complex digital-signal processor can be used to process the image.

1.2 Thesis Contribution

An ideal per-column DSM ADC for a CMOS image sensor is a DSM ADC that has a transistor function that is linear and robust to any gain or offset error cause by transistor voltage-threshold mismatch or capacitor ratio mismatch. This thesis looks at and examines the drawbacks and advantages of different types of per-column DSM

ADCs that can be used in a CMOS imager. It also examines the transfer function of each architecture and determines the architecture robustness to gain and offset errors caused by voltage-threshold mismatch.

This thesis also introduces a DSM ADC architecture in which the transfer function is robust to any gain and offset errors caused by transistor voltage-threshold mismatch. This DSM ADC is an upgrade to the DSM ADC architecture that was introduced by Montierth [1]. Montierth's DSM ADC has a transfer function that is robust to offset errors but sensitive to gain errors.

1.3 Various CMOS Pixel Architectures

There are many types of CMOS pixel architectures but the basic operation of each type of pixel is similar. All CMOS pixels use a photodiode that converts light energy into an electrical signal that can be measured using an analog-to-digital converter. The photodiode is initially set to a reverse-biased configuration. As the photon hits the photodiodes, electron-hole pairs are generated in the photodiode. This neutralizes the charge stored on the reverse-biased photodiode as shown in Figure 1.1. As the charge on the photodiode is neutralized, the voltage across the reverse-biased photodiode is reduced. This change in voltage will be converted to a digital code by an ADC. Five different types of CMOS pixel architecture will be discussed in this introduction: Passive Pixel, PIN Photodiode-type active pixel sensor (APS), Pinned Photodiode-type APS, Photogate-type APS, and Logarithmic APS.

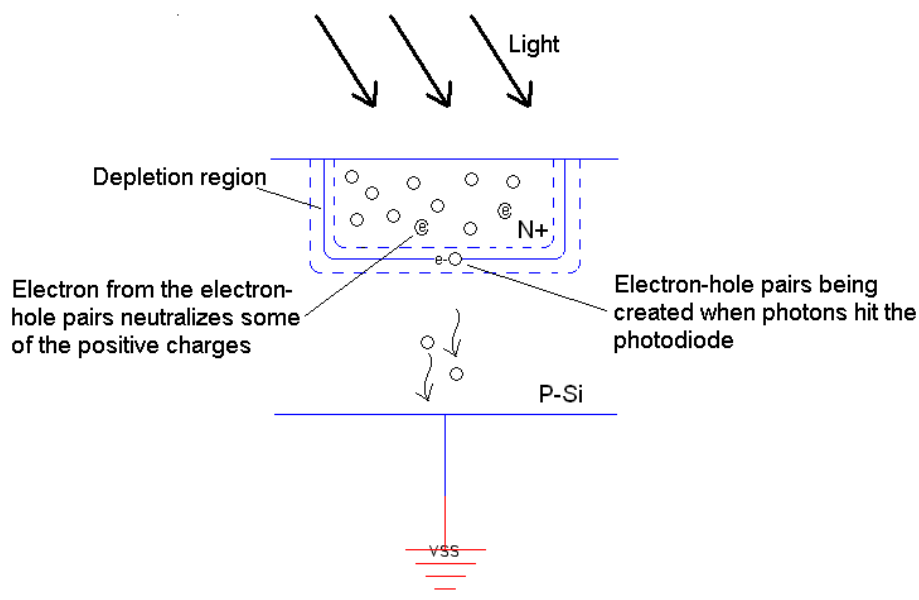


Figure 1.1 Diagram showing the charge stored on the photodiode is being neutralized when it is exposed to light.

1.3.1 The Passive Pixel

The passive pixel architecture consists of a photodiode and a transistor; as shown in Figure 1.2. A column of these pixels are connected in parallel and their column line node is shared among one another as shown in Figure 1.3. The TX signal is the row line access signal and is shared between pixels on the same row.

Initially, the column bus voltage will be stored at the cathode terminal of the photodiode. As photons strike the photodiode, electron-hole pairs will be created to neutralize some of the charge stored across the reverse-biased photodiode. The photodiode will remain disconnected from the column line until a voltage pulse is sent to

the TX node. This period of exposure to light is known as aperture time. The greater the intensity of the light, the voltage drop across the photodiode will be larger. When the access transistor is turned on, the photodiode will then connect to a charge integrating amplifier (CIA) at the bottom of the column line to reset the voltage of the photodiode to the column bus voltage as shown in Figure 1.4. As the charge-integrating amplifier resets the voltage across the photodiode, it will also convert the remaining charge stored on the photodiode into a voltage signal. This voltage signal will then be converted to a digital signal by means of an analog-to-digital converter.

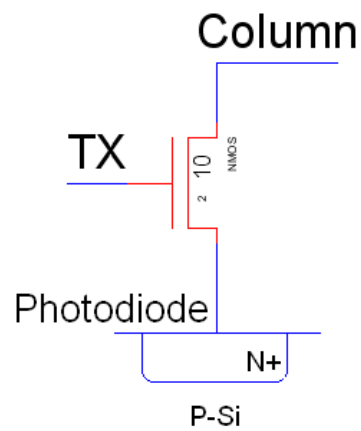


Figure 1.2 A schematic diagram for a CMOS passive pixel [3].

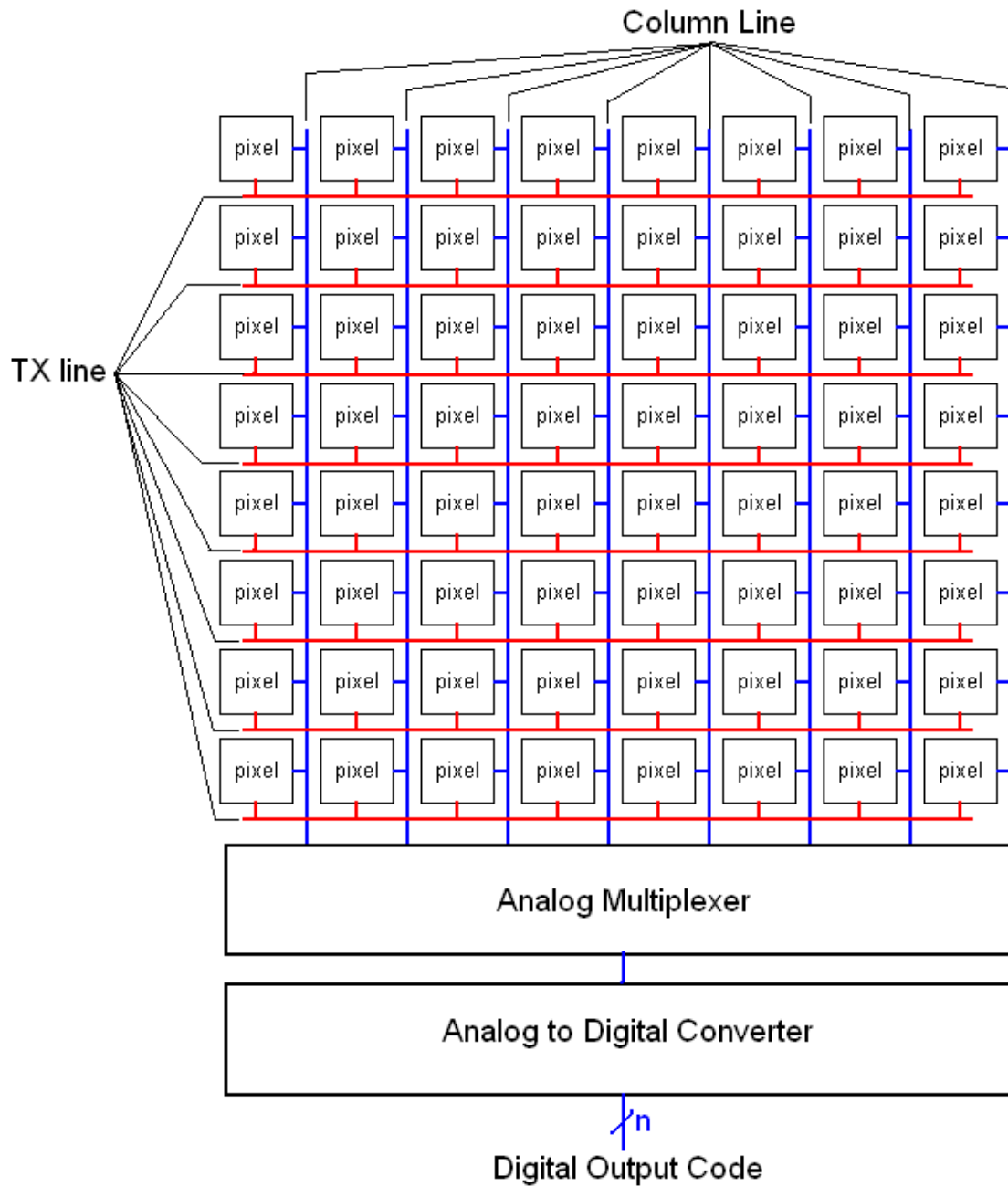


Figure 1.3 A layout diagram of an 8 by 8 pixel array.

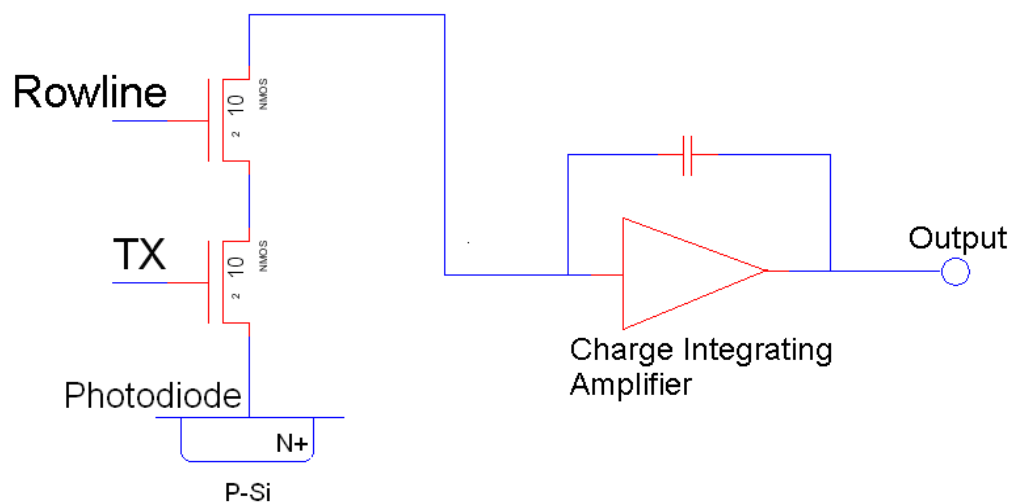


Figure 1.4 A schematic diagram for a passive pixel CMOS imager with a charge integrating amplifier [4].

Since only one transistor is required for each pixel, the fill rate factor for this architecture is very high (the amount of pixels per square area is high). However, noise is the biggest obstacle for the success of this architecture. Since the cathode terminal of the photodiode is not buffered from the column line, a noisy and highly capacitive (when the column line is long and contains a large number of pixels) column line might generate noise that will influence the signal voltage stored on the cathode terminal of the photodiode. The readout noise is approximately 250 electrons RMS [3]. The passive pixel is also not scalable when fast readout is needed [3]. As the density of the pixels increase, the column line's parasitic capacitance increases. Since the pixel is connected directly to the column line, a fast readout will not be possible for a long and capacitive column line.

1.3.2 PIN Photodiode-Type APS

The main difference between an active and passive pixel is that the photodiode in an active pixel is buffered from the column line, whereas the photodiode in a passive pixel is not. Figure 1.5 shows the schematic diagram of a PIN photodiode-type APS. As compared with Figure 1.2, the photodiode is buffered from the column line through the NMOS source follower, M2. This source follower also helps maintain good signal linearity between the voltage on the floating diffusion and the column line by providing isolation.

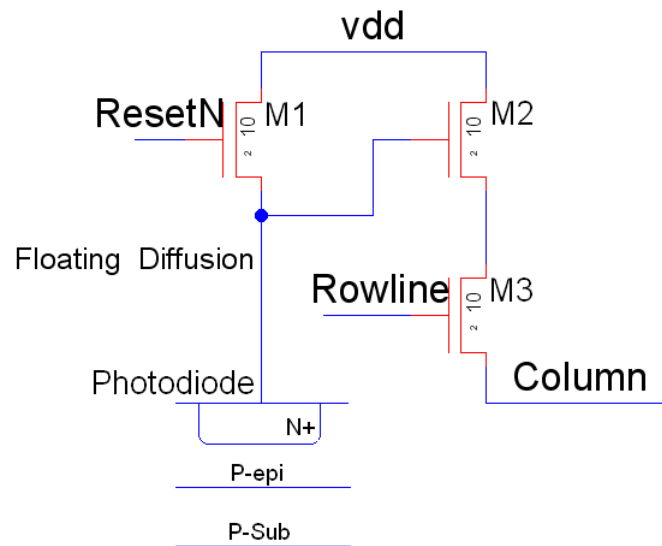


Figure 1.5 Schematic diagram for the photodiode-type APS [3].

Like the passive pixel sensor, this pixel sensor is also laid out in the same manner, where the TX signal in the Passive Pixel architecture is now the Rowline signal in the PIN Photodiode-type APS. The column line is also shared with other pixels on the same column.

A PIN photodiode is a photodiode that consists of 3 layers: a p^+ substrate, a p-epi layer, and a n^+ diffusion [5]. Figure 1.6 shows a cross-section image of an OmniVision OV3610 PIN photodiode [5]. The n^+ diffusion serves as the cathode terminal of the photodiode and it is connected to the reset transistor (this node is known as the floating diffusion). On the other hand, the p-epi layer is a shared terminal across all pixels. It is connected to ground.

Using a standard photodiode will only yield a monochrome image. Red, green, and blue color filters can be placed on top of the PIN photodiode to detect the image in color. Instead of using color filters, Foveon introduced a pixel technology that detects the red, green, and blue light by the depth of the n^+ diffusion in the p-epi layer [5].

The blue light can be detected by placing the n^+ diffusion at the top of the P-epi layer with a thickness of $0.1\mu\text{m}$. An n^+ diffusion that is approximately $0.9\mu\text{m}$ to $1.6\mu\text{m}$ down with a thickness of $0.65\mu\text{m}$ can be used to detect green light. While the red light can be detected with an n^+ diffusion that is located $2.7\mu\text{m}$ to $3.5\mu\text{m}$ below the p-epi layer. The thickness of this red-light detecting diffusion is $0.95\mu\text{m}$. Figure 1.7 shows the cross-section profile of a PIN photodiode used in Foveon image sensors to detect the three distinct colors of light through the depth of the n^+ diffusion [5]. With this technology, three color photodiodes can be placed in a single pixel, which increases the fill rate.

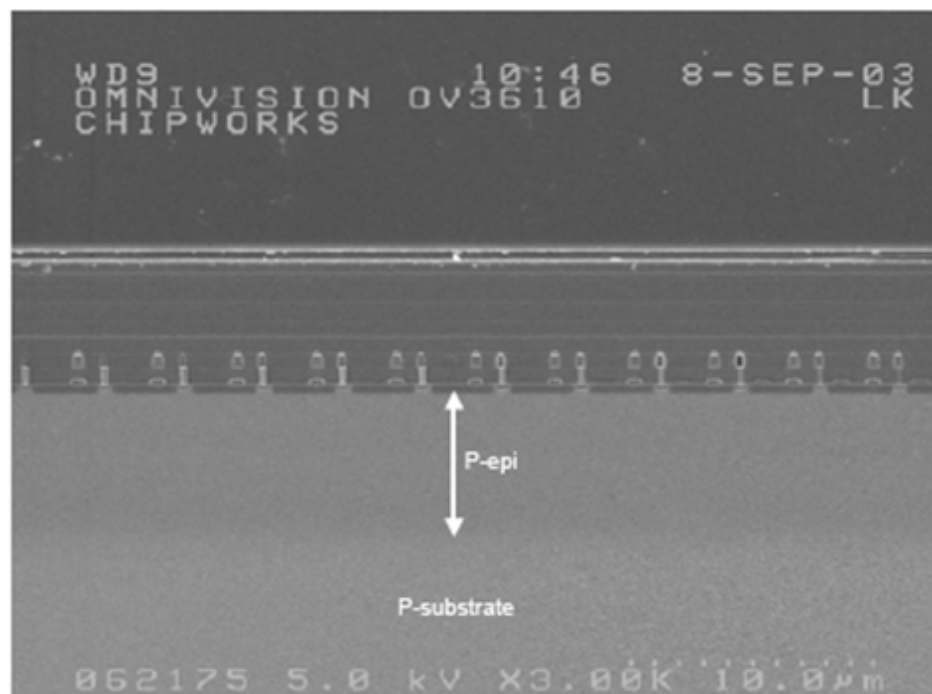
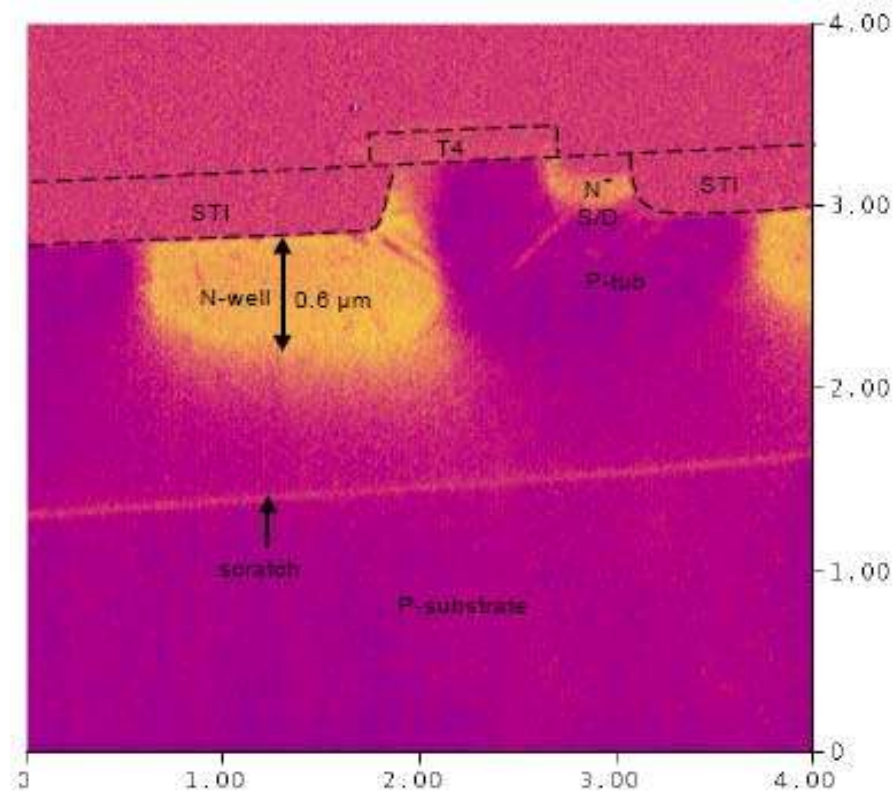


Figure 1.6 A cross-section image of a PIN photodiode.

Referring back to Figure 1.5, to begin detecting the image signal, the ResetN signal will go high, turning on the reset transistor, M1, and resetting the voltage on the cathode terminal to a reference voltage, V_{ref} , that is sometimes set to V_{DD} . The voltage on the cathode of the photodiode will be sampled onto a reference-hold capacitor through M2, M3, and the column line. Following this, the reset transistor will be turned off by driving the ResetN signal low. The photodiode will then begin generating electron-hole pairs and neutralizing the charge on the cathode terminal of the photodiode. After a certain aperture time, the voltage across the photodiode (or voltage on the cathode of the photodiode) will be sampled onto the image-hold capacitor.

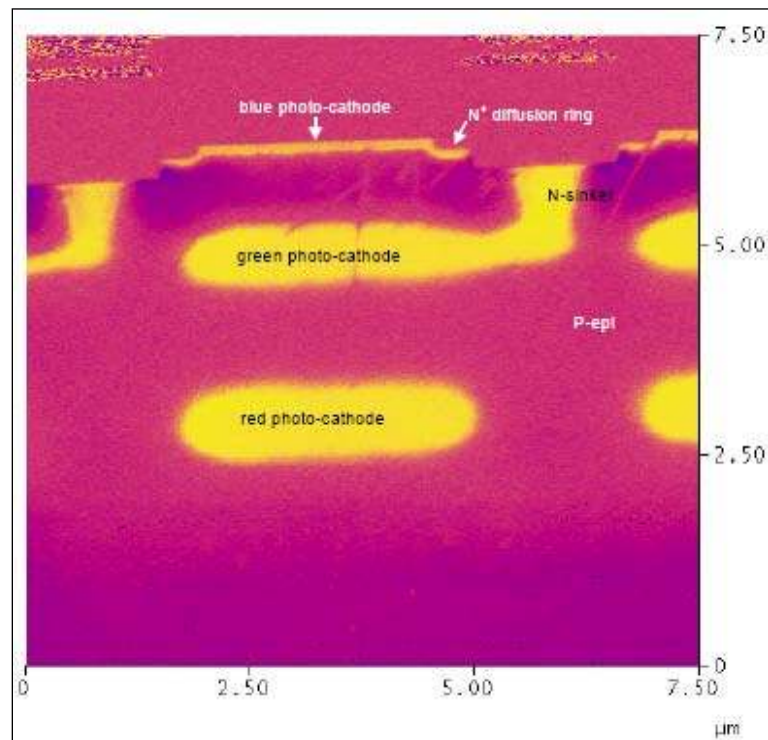


Figure 1.7 A SCM cross-section profile of the photo-cathodes in the Foveon F018-50-F19A.

If the source-follower transistor, M2, is not identical among all the pixels in the imager array, the voltage sampled on the hold capacitors will be different from other pixels due to M2 voltage-threshold mismatch. This error is known as fixed-pattern noise (FPN). Fixed-pattern noise can be reduced through the means of correlated double sampling (CDS). Correlated double sampling is discussed in greater detail later.

The APS seen in Figure 1.5 is more robust to column noise than the APS seen in Figure 1.2. In addition, it's scalable for faster readout since the photodiode is now buffered from the column line. With CDS, additional flicker noise can be removed. The main noise contribution in this circuit is the reset noise (if correlated double sampling is not used) on the photodiode. Usually, this noise is in the range of 75 to 100 electrons RMS [3].

The PIN photodiode has higher conversion gain than the passive pixel sensor because the photodiode capacitance is separated from the column parasitic capacitance. This APS provides an additional robustness to noise at the expense of area or fill factor rate. A minimum of three transistors are needed for this architecture, resulting in a pixel size of approximately 15 times the feature size.

1.3.3 Pinned Photodiode-Type APS

The pinned photodiode-type APS architecture is very similar to the PIN photodiode-pixel sensor; see Figure 1.8.

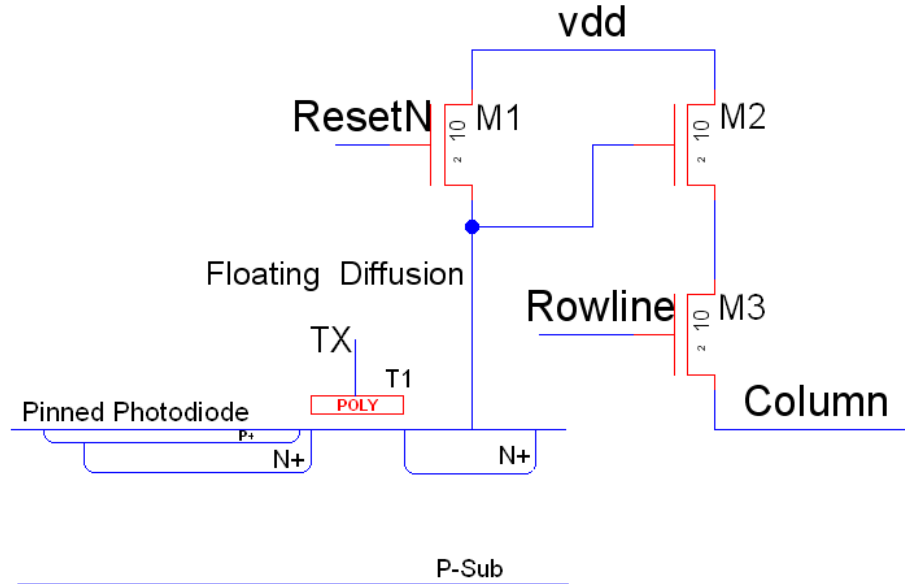


Figure 1.8 A diagram of a pinned photodiode pixel sensor [3].

A pinned photodiode is a shallow p-n junction that is adjacent to a transfer transistor. The p⁺ implant will be approximately 0.2 μ m deep and cover the n⁺ diffusion that is approximately 0.6 μ m deep. The n⁺ diffusion extends slightly past the p⁺ diffusion so that it makes a connection with the transfer-gate transistor, T1 in Figure 1.8. From Figure 1.8, the p⁺ implant's Fermi level is pinned by the n⁺ diffusion (the Fermi level is pinned around the p+ implant). This is to allow the photodiode to completely empty its collected charge when TX is pulsed, else an image “lag” will occur [6]. Figure 1.9 shows a cross-section view of a Canon EOS 10D pinned diode APS [5].

The floating diffusion will be set to a known reference voltage (sometimes *VDD*) when the reset transistor, M1, is turned on. This voltage is then sensed and stored on a reference-hold capacitor through the source-follower transistor, row-line access transistor

and column line. The voltage stored on this capacitor is the sum of the reference signal, noise, and voltage mismatches.

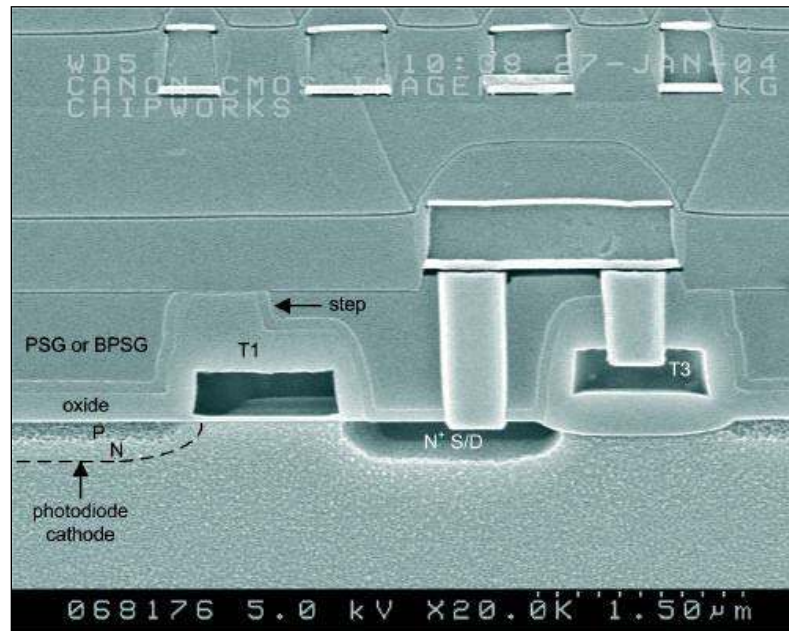


Figure 1.9 An image of a pinned-photodiode.

While the floating diffusion is set to a reference voltage, the pinned photodiode collects the photon and convert the energy into charge. The amount of charge stored in the pinned-photodiode increases (integrates) over time. After a certain aperture time, the charge stored is transferred to the floating diffusion by turning on the transfer-gate transistor, T1. This voltage is then transferred to an image-hold capacitor through the same path as the reference signal (source-follower transistor, row-line access transistor, and column line). Just like the reference signal, the voltage stored on this capacitor is the sum of the image signal, noise, and voltage mismatches.

When using correlated double sampling (CDS), an autozero operation followed by a sample-and-hold operation, the voltage on the image capacitor is subtracted from the voltage of the reference capacitor (autozero process), yielding an output signal that has reduced low-frequency noise and is free from DC voltage mismatches. The result is a reduction in fixed-pattern noise.

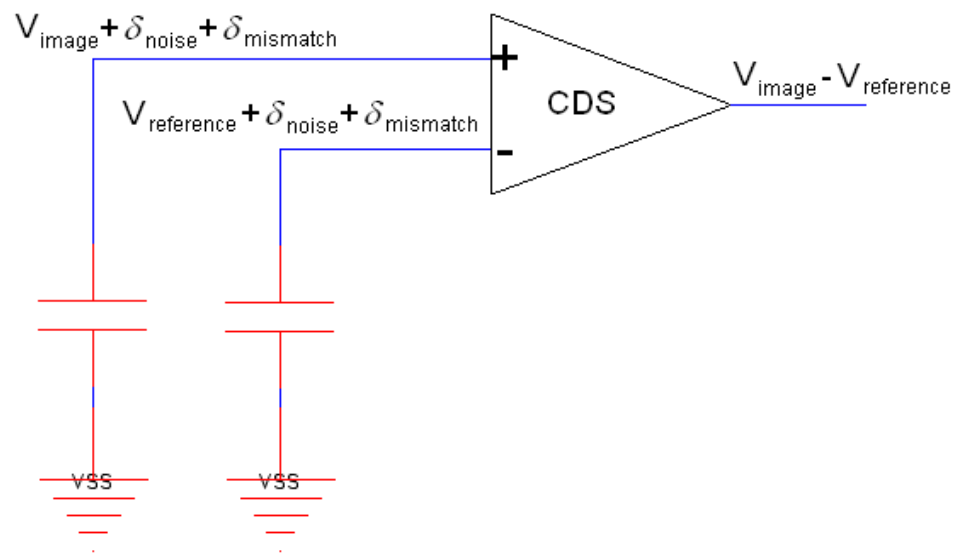


Figure 1.10 A diagram showing the output of a CDS is free of noise and voltage mismatches.

This pinned-photodiode structure allows the image signal to be integrated at the same time the reference signal is being sampled onto the reference-hold capacitor. As compared to the PIN-photodiode structure, the image signal integration “session” cannot take place in parallel with the sampling of the reference signal because the transfer gate transistor does not exist in the photodiode structure. Therefore, this pinned-photodiode

structure will be able to cancel higher frequency noise better than other photodiode structures since the time between the sampling of image and reference are closer together.

The minimum number of transistors needed for this structure is four. Therefore, the fill-factor rate for this architecture is less than the PIN photodiode structure. In the PIN photodiode structure, the 3 color (red, green, and blue) can be sensed using one pixel but with different depths of n+ diffusion. However, the pinned diode cannot use this same technology. With three different photodiodes, each one needs its own color filter to capture the three light wavelength ranges. Therefore, three times more area will be needed for capturing the image in color.

1.3.4 Photogate-Type APS

The photogate-type APS was introduced in 1993 for high-performance scientific and low-light applications [3]. Figure 1.11 shows the basic circuit diagram for a photogate APS.

The operation of the photogate pixel sensor is very similar to the pinned photodiode pixel sensor. The transfer gate, TX, is not connected to a voltage signal but it is fixed to some reference voltage, normally $VDD/2$. The photogate node, PG, will be set to VDD when the reference signal is being sampled onto the reference hold capacitor. Instead of taking the TX node to VDD to dump the charge from the photodiode to the floating diffusion, the photogate node, PG, will pulse from VDD to ground; the image

signal is sampled onto the image hold capacitor. Correlated double sampling may be done on the image and reference signal to reduce noise and systematic offsets.

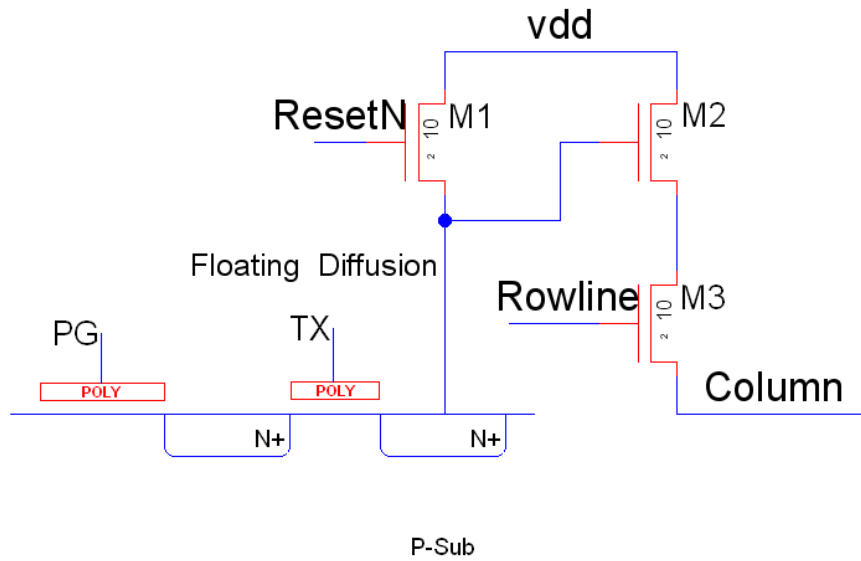


Figure 1.11 Schematic diagram of a photogate APS [3].

The photogate structure requires a minimum of 4 transistors that translates to a pixel size of approximately 20x the feature size. The benefit of noise reduction is at the cost of a reduction in fill-rate factor as compared to the PIN photodiode structure. Just like the pinned photodiode, 3 different color pixels (red, green, and blue) are needed to detect a color image.

1.3.5 Logarithmic APS

In some applications, a nonlinear pixel sensor is desired. This pixel generates a logarithmic output signal with respect to its photo signal [3]. The logarithmic APS

structure is like the photodiode APS but its ResetN signal is tied to VDD . Figure 1.12 shows the schematic diagram of a logarithmic APS.

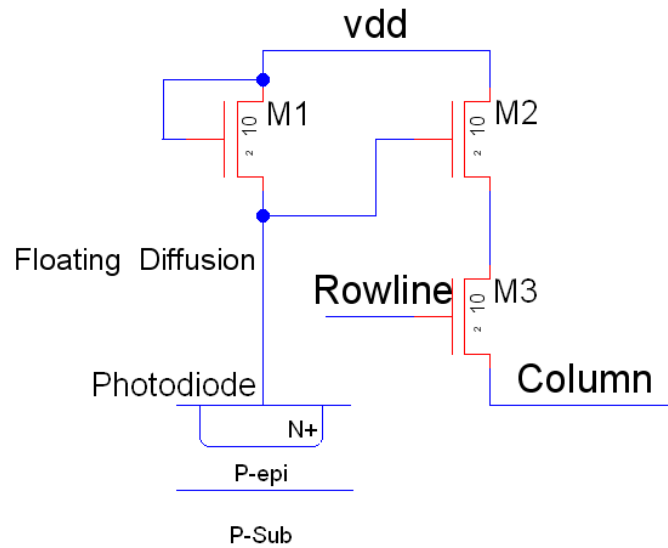


Figure 1.12 Schematic Diagram of a standard logarithmic APS [3].

The reset transistor, M1, now operates in the sub threshold region since the gate is tied to its drain. The voltage on the source of the “weak” transistor, M1, will never be greater than $VDD - V_{th,weak}$. As light hits the photodiode, charge will be generated and stored on the cathode terminal. This charge will lower the voltage of the source of M1 and turn the M1 transistor slightly on. Some of this charge will try to escape or flow from the source to VDD through M1. A constant current will be generated when photons hit the photodiode. Since transistor M1 operates in the sub threshold region (a logarithmic I-V relationship curve), the output from this pixel is also then logarithmic.

This logarithmic pixel structure suffers from fixed pattern noise and systematic offset because CDS cannot be used in this design. The reference voltage is never

sampled. This pixel sensor also suffers from poor response time in low light environment and low signal-to-noise ratio because it is a non-integrating approach. Also, the systematic offset is not cancelled.

1.4 An Overview of the Use of Correlated Double Sampling in an APS

Correlated double sampling is used in most APS to help reduce low-frequency noise and offsets. Initially, the reset transistor, M1, will be turned on by taking the signal ResetN high. This will set the voltage on the floating diffusion node, N_{float} , to a reference voltage, which is often VDD . This reference voltage is also sometimes known as V_{RESET} .

This V_{RESET} signal will then propagate through the source follower, M2, and the row-line access transistor, M3, onto the column line. The signal on the column line will not be V_{RESET} but:

$$V_{RESET,column} = V_{RESET} + V_{os} \quad (1-1)$$

This offset voltage, V_{os} , is due to voltage-threshold offset and mismatches from the source follower transistor.

Once the $V_{RESET,column}$ is stable on the column line, the M_{SHR} transistor is turned on to allow the reference voltage to be sampled onto the reset hold capacitor, C_{HR} . However, the M_{SHR} transistor cannot be left on for a long time because the $1/f$ flicker noise will be integrated yielding a noisier sampled reference voltage. The time it stays on should just

be sufficient for the capacitor to stabilize to the reference signal voltage. The final voltage signal sampled onto the reference hold capacitor is:

$$V_{RESET,CHR} = V_{RESET} + V_{os} + V_{error,switch,t=1} + V_{noise,t=1} \quad (1-2)$$

When signal SHR goes low, the clock feed through and charge injection from M_{SHR} is also sampled and it is labeled as $V_{error,switch,t=1}$. The flicker and thermal noise from transistor $M1$, $M2$, $M3$, and M_{SHR} are also sampled and it is labeled as $V_{noise,t=1}$.

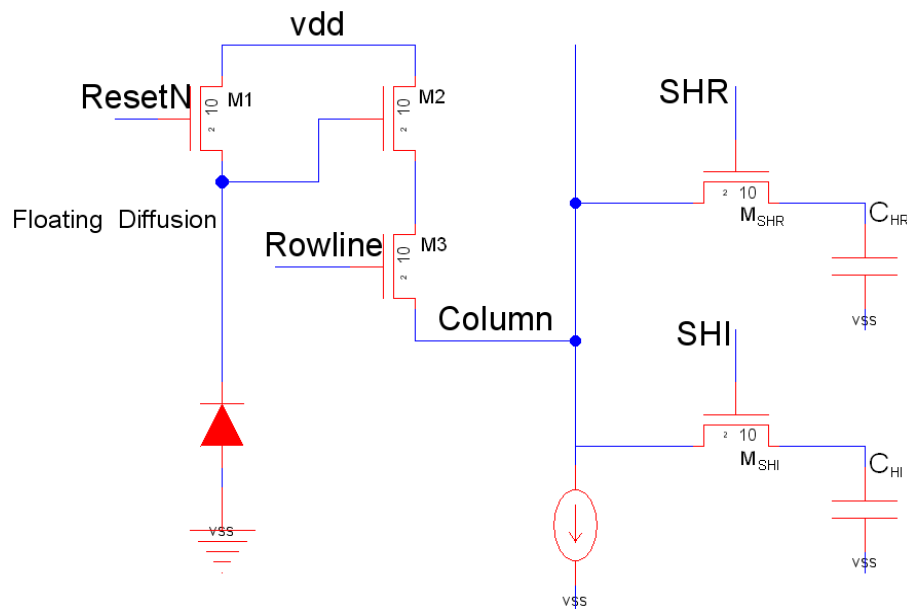


Figure 1.13 Schematic used to illustrate correlated double sampling.

As soon as SHR goes low, ResetN will turn off allowing the photodiode to integrate the image signal on the floating diffusion, N_{float} . This image signal, V_{IMAGE} , will propagate through $M2$ and $M3$ to the column line. Just like the reference signal, the voltage on the column line will not be V_{IMAGE} but:

$$V_{IMAGE,column} = V_{IMAGE} + V_{os} \quad (1-3)$$

Once the signal on the column line is stable and after a set aperture time, M_{SHI} is turned on just long enough for the image hold capacitor, C_{HI} , to charge up to the column line voltage. The voltage sampled on the image hold capacitor after the SHI signal goes low is:

$$V_{IMAGE,CHI} = V_{IMAGE} + V_{os} + V_{error,switch,t=2} + V_{noise,t=2} \quad (1-4)$$

$V_{error,switch,t=2}$ is the clock feed through and charge injection error when sampling the image signal onto the image hold capacitor. On the other hand, $V_{noise,t=2}$ is the flicker and thermal noise from transistor M1, M2, M3, and M_{SHI} .

If the size of M_{SHR} and M_{SHI} is the same and the SHR and SHI have approximately the same fall time, then $V_{error,switch,t=1}$ is about the same as $V_{error,switch,t=2}$. $V_{noise,t=1}$ and $V_{noise,t=2}$ are flicker and thermal noise from the photodiode and transistor M1, M2, M3, and M_{SHx} (M_{SHR} for reference signal and M_{SHI} for image). If the time between sampling the reference and image signal is short (or the aperture time is small), $V_{noise,t=1}$ and $V_{noise,t=2}$ will be approximately the same. The offset, V_{os} sampled with both the image and reference signals is the same since it is the same voltage-threshold mismatch on the source follower transistor, M2.

Once both the image and reference signals are sampled, both signals will be fed into a fully differential ADC (e.g., a Delta-Sigma-Modulator). The net differential input signal sent to the ADC is

$$V_{ADC,diff} = (V_{IMAGE} + V_{os} + V_{error,switch,t=2} + V_{noise,t=2}) - (V_{RESET} + V_{os} + V_{error,switch,t=1} + V_{noise,t=1}) \quad (1-5)$$

$$V_{ADC,diff} = (V_{IMAGE} - V_{RESET}) + (V_{error,switch,t=2} - V_{error,switch,t=1}) + (V_{noise,t=2} - V_{noise,t=1}) \quad (1-6)$$

$$V_{ADC,diff} = (V_{IMAGE} - V_{RESET}) + \delta_{error,switch} + \delta_{noise} \quad (1-7)$$

$\delta_{error,switch}$ is zero if the size of M_{SHR} and M_{SHI} is the same and SHR and SHI have the same fall time. δ_{noise} is small and negligible if the aperture time is short.

Therefore, the measured differential voltage by the ADC is

$$V_{ADC,diff} = (V_{IMAGE} - V_{RESET}) \quad (1-8)$$

From Equation 1-8, we can see that the net input signal to the ADC can be approximated to simply the image signal minus the reference signal. This means that the output of a noiseless ADC with an ideal photodiode will be free from fixed-pattern noise and random noise like flicker and thermal.

CHAPTER 2: CMOS IMAGE SENSOR USING A DELTA-SIGMA ADC

2.1 An Analogy for the Delta-Sigma Modulator

A Delta-Sigma Modulator ADC can be described with the help of Figure 2.1.

Let's assume that the measured voltage is the water level in the Measuring Bucket. The float in the measuring bucket controls the water flow out of the Sigma Bucket. If the water level in the Measuring Bucket is relatively large then the water that flows out of the Sigma Bucket is relatively large. On the other hand, if the water level in the Measuring Bucket is relatively low, the water that flows out of the Sigma Bucket is relatively smaller.

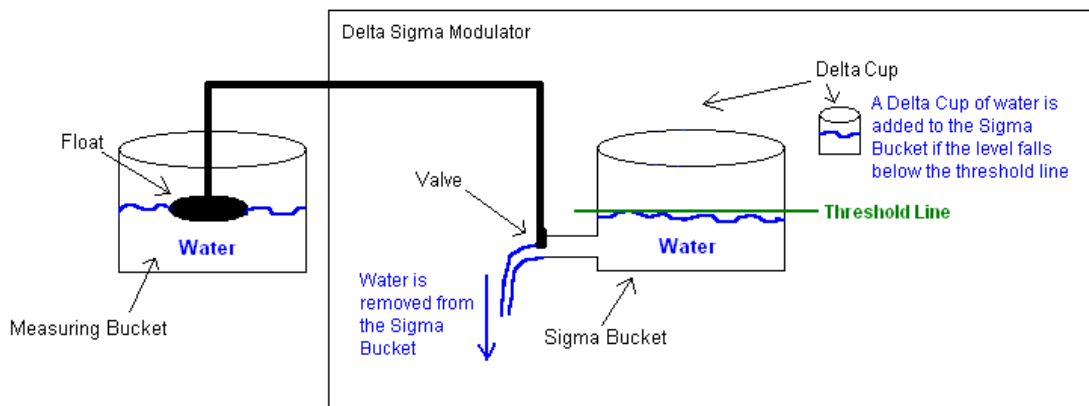


Figure 2.1 A picture that demonstrates the general idea of a DSM ADC.

When the water level in the Sigma Bucket drops below some arbitrary threshold line, a Delta Cup of water will be added to the Sigma Bucket. This addition is counted

and recorded. If the water level in the Measuring Bucket is high, the water will flow out of the Sigma Bucket at a fast rate and the number of times that a Delta Cup of water is added per unit time will increase. On the other hand, if the water level in the Measuring Bucket is low, the water flowing out of the Sigma Bucket will be slower and the number of times that a Delta Cup of water is added per unit time will decrease.

From this analogy, the water level in the Measuring Bucket can be determined by averaging the number of times that water is added to the Sigma Bucket by the Delta Cup.

2.2 Sensing Scheme for a DSM in a CMOS Image Sensor

Figure 2.2 illustrates the sensing scheme used by a DSM in a CMOS Image Sensor. There is one DSM for each column of pixels and the sensing occurs in parallel for each column.

The sensing scheme begins with sampling the pixel's reset signal onto the reset sample and hold capacitor, C_{HR} . This is accomplished by turning on the rowline and ResetN signals on one of the multiple rows of pixels in the array. Each pixel on the activated row will output its reset signal onto its respective column line. This reset signal is then sampled onto the C_{HR} capacitor through the activated SHR switch. Once the reset signal is sampled, the rowline, ResetN, and SHR switches are turned off.

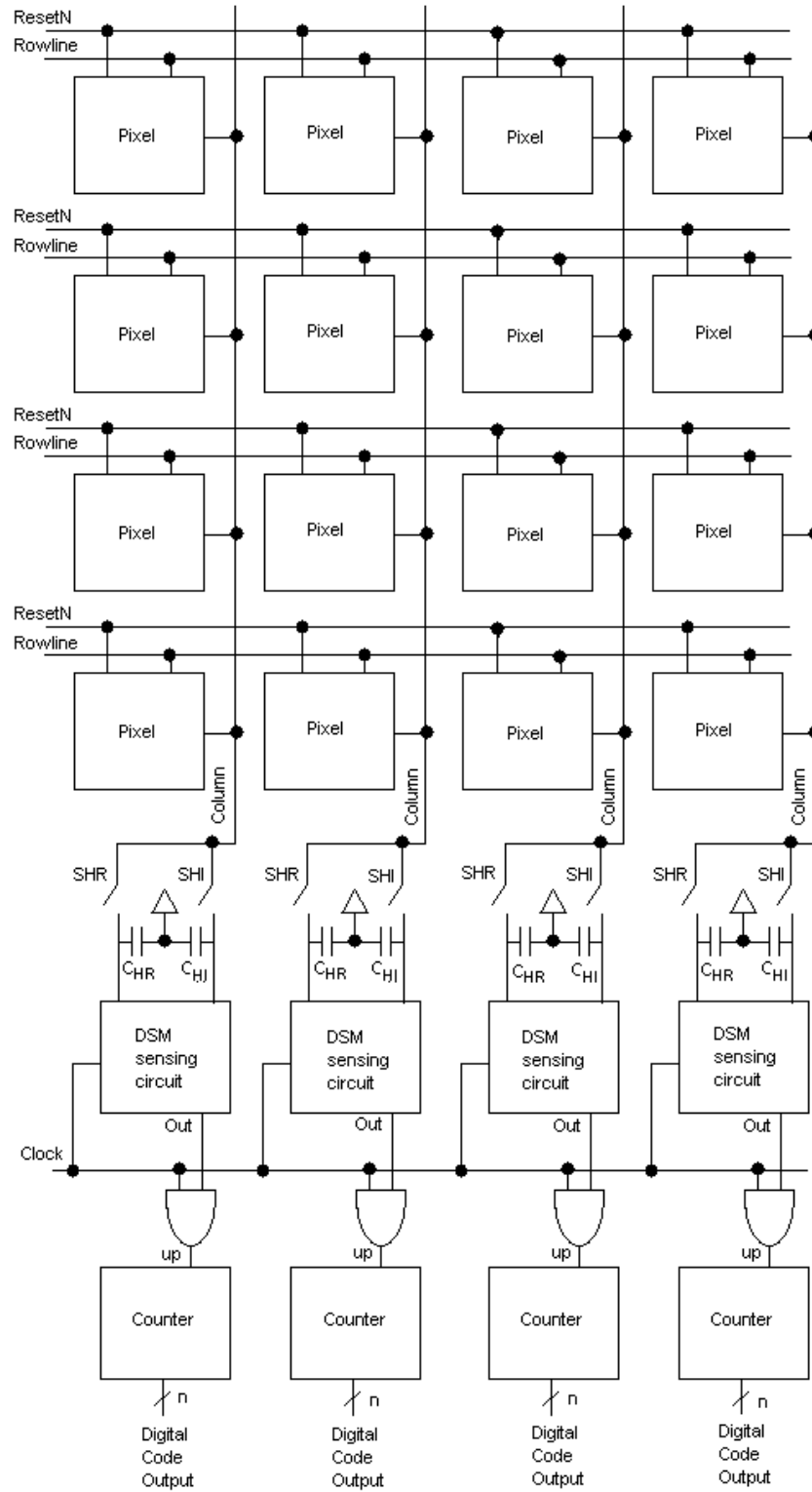


Figure 2.2 A 4x4 pixel diagram of a DSM CMOS Imager.

After the reset signal is sampled, the pixel is then exposed to light for a length of time. Once the exposure time has expired, the same rowline and SHI switch is turned on. This samples the image signal onto the image sample and hold capacitor, C_{HI} . The rowline and SHI switch is turned off once the image signal is sampled onto C_{HI} .

Next, the DSM will take the reset and image input signals that were sampled on the two C_H capacitors and convert them to a digital code equivalent. The n-bit wide counter that is connected at the end of the DSM will help the DSM convert the analog input signals to a digital output code.

2.3 DSM Operation in a CMOS Image Sensor

Figure 2.3 shows the schematic diagram of a basic DSM sensing circuit in a CMOS Image sensor [2]. The differential input signals, image (V_{IMAGE}) and reset (V_{RESET}) are stored on the two different sample-and-hold capacitors that are connected to the gates of the PMOS transistors M7 and M8 respectively. These transistors serve the purpose of a source follower for the input signals. The transistors convert the input voltages into current sets that flows into the sigma bucket. The voltage levels on the sources of the M7/M8 source-followers are equal to the gate voltage plus a threshold as long as the width of the source-follower transistors, M7 and M8 are large. This relationship can, and will, be derived now. These source-followers are operating in the saturation region. The equations governing their operation are

$$I_{M7,M8} = \frac{\mu_p C_{ox} W_{M7,M8}}{2L_{M7,M8}} (V_{sM7,M8} - V_{gM7,M8} + V_{thM7,M8})^2 \quad (2-1)$$

where:	$I_{M7,M8}$	Drain Current for transistor M7 and M8 (A)
	μ_p	Surface Mobility for the P-channel Transistor (cm ² /Vs)
	C_{ox}	Oxide Capacitance (fF/μm ²)
	$W_{M7,M8}$	Width of transistor M7 and M8 (μm)
	$L_{M7,M8}$	Length of transistor M7 and M8 (μm)
	$V_{sM7,M8}$	Source voltage of transistor M7 and M8 (V)
	$V_{gM7,M8}$	Gate voltage of transistor M7 and M8 (V)
	$V_{thM7,M8}$	Threshold voltage of transistor M7 and M8 (V)

By rearranging the variables in Equation 2-1, the equation relating the source voltage to the gate voltage is given in Equation 2-2 (seen below). If the width-to-length ratio for transistors M7 and M8 is large, Equation 2-2 can be simplified into Equation 2-4. This reduction shows the voltages on the sources of transistors M7 and M8 are simply the sum of the input gate voltages and the PMOS threshold voltage.

$$V_{sM7,M8} = V_{gM7,M8} + V_{thM7,M8} + \sqrt{\frac{2L_{M7,M8}I_{M7,M8}}{\mu_p C_{ox} W_{M7,M8}}} \quad (2-2)$$

$$V_{sM7,M8} = V_{gM7,M8} + V_{thM7,M8} + \delta_{w,error} \quad (2-3)$$

$$V_{sM7,M8} \approx V_{gM7,M8} + V_{thM7,M8} \quad (2-4)$$

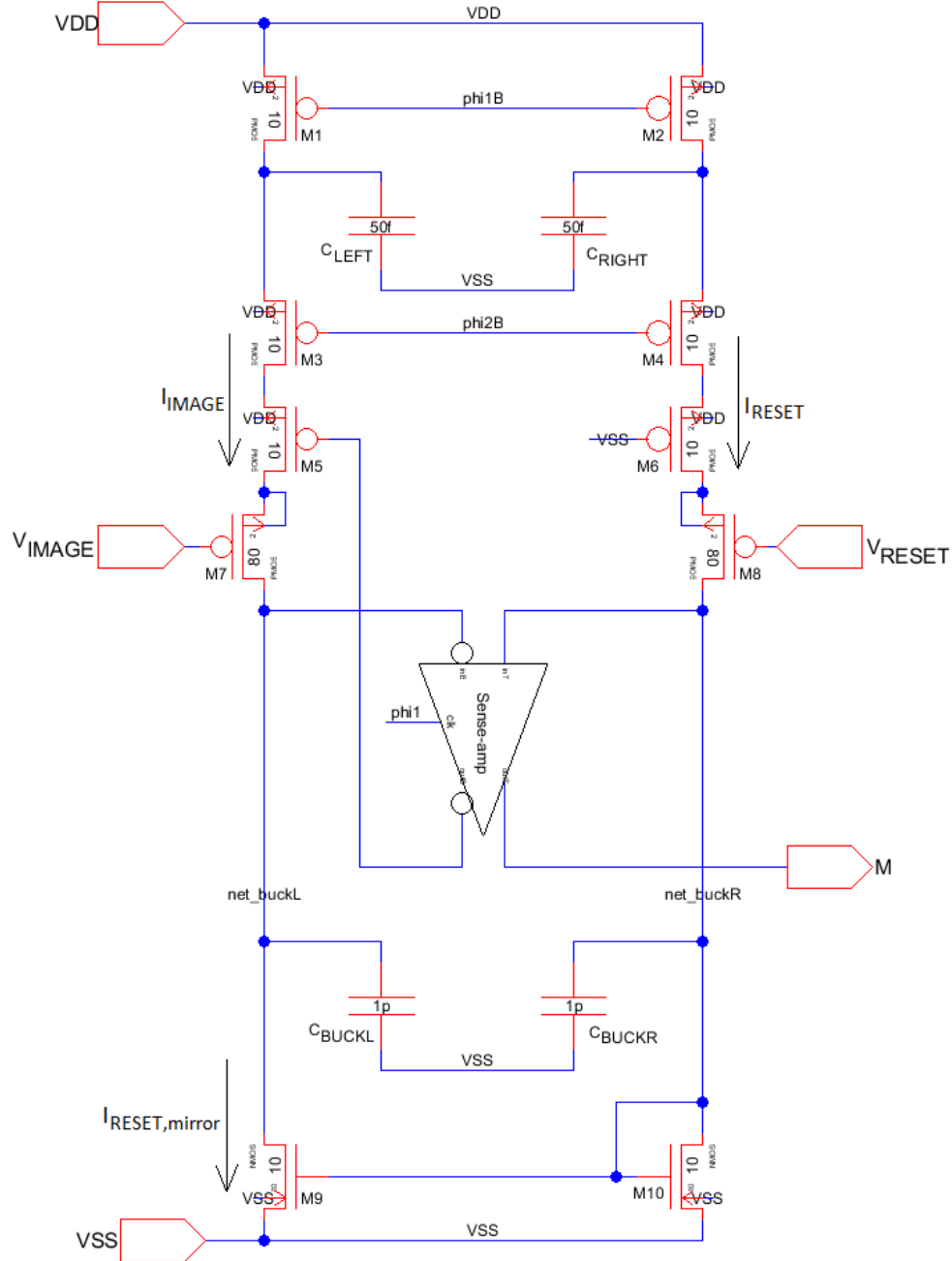


Figure 2.3 Schematic of a Basic CMOS Imager Delta Sigma Modulator [2].

Simulations can be used to determine the optimal widths for the source follower transistor so that the width error, $\delta_{w,error}$, is minimized. A DC sweep simulation is run on

the schematic shown in Figure 2.4. A total of 5 transistor sizes were simulated: 20λ ($1.2\ \mu\text{m}$), 40λ ($2.4\ \mu\text{m}$), 60λ ($3.6\ \mu\text{m}$), 80λ ($4.8\ \mu\text{m}$), and 100λ ($6.0\ \mu\text{m}$). The VDD terminal is set to 5V and the VSS terminal is connected to ground. The vin signal is swept from 5V to 0V.

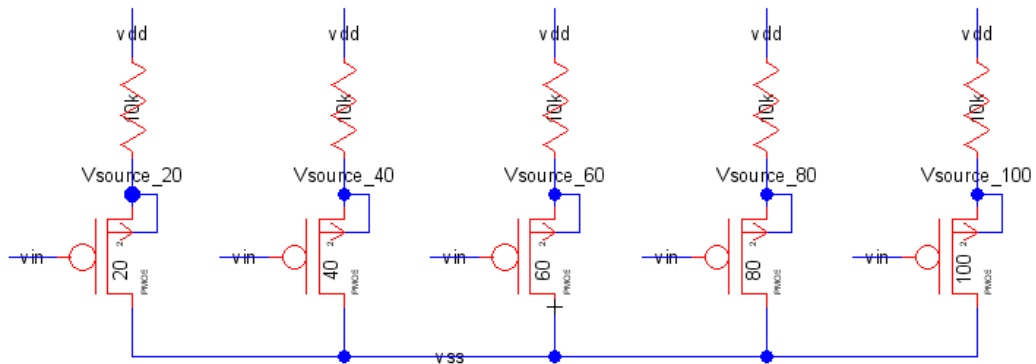


Figure 2.4 Schematic to determine the optimum source-follower transistor size.

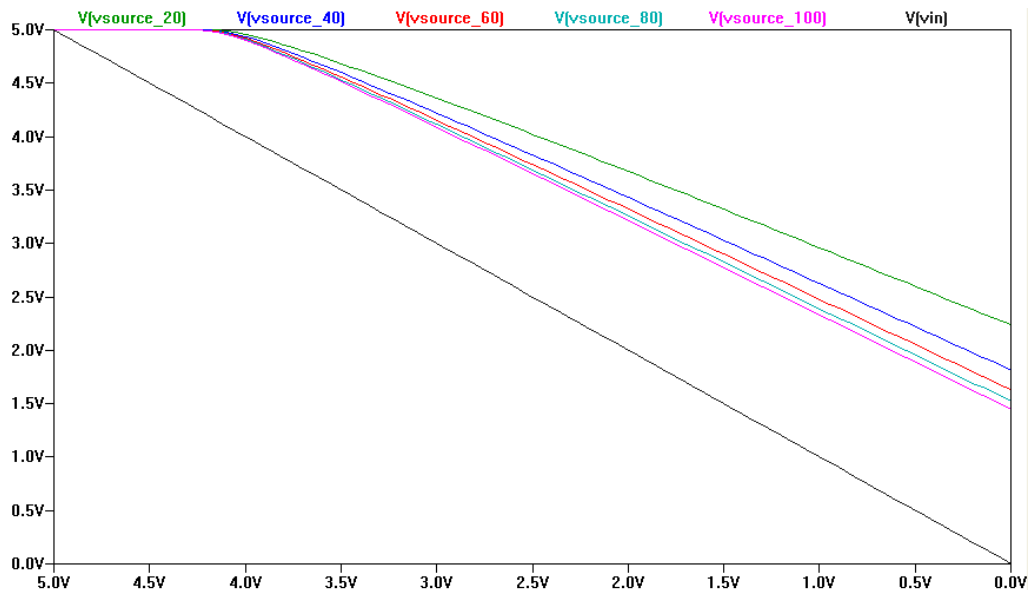


Figure 2.5 A DC sweep on the five PMOS source follower-transistor in Figure 2.4 with its source terminal as the output.

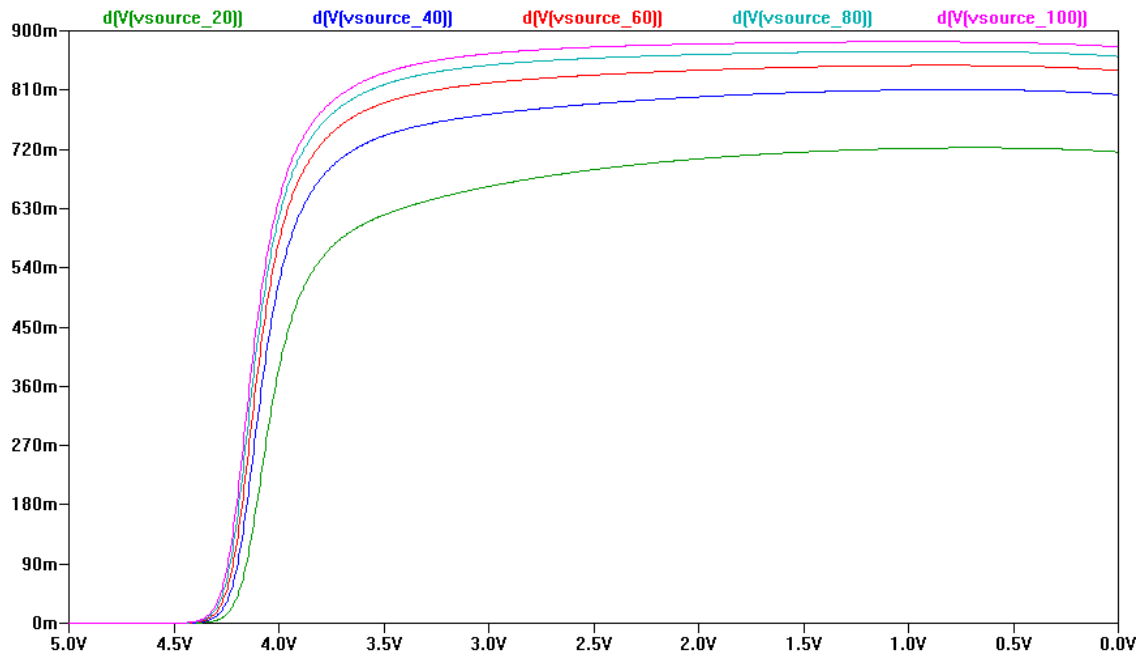


Figure 2.6 The slope of the source terminal (output) for the DC sweep simulation on the five PMOS source-follower transistors in Figure 2.4.

From Figure 2.5, the PMOS source-follower with a width of 20λ does not track well with the input signal, v_{in} . As the v_{in} signal approaches 0V, the source voltage on the PMOS moves away from the v_{in} signal. When the width of the source-follower increases to 40λ , the source voltage diverts less when the input signal approaches 0V. This diversion reduces as the width of the PMOS transistor increases. This is because the slope of the source terminal changes less as the width of the transistor increases, as shown in Figure 2.6. The source-follower with a width of 20λ has the greatest slope changes and the source-follower with a width of 100λ has the least slope changes. The slope changes for the source terminal between the 80λ and 100λ transistors are fairly similar. Therefore,

a width of 80λ or $4.8\mu\text{m}$ for the PMOS source-follower is adequate for this DSM (as shown in Figure 2.3).

The PMOS source-followers in Figure 2.3, M7 and M8, have the body terminals tied to their source terminals. This configuration is necessary because it eliminates any source to body voltage, V_{sb} , dependency in the threshold voltage. In other words, this connection removes body-effect in these MOSFETS. Equation 2-5 shows the relationship between the threshold voltage and source-to-body voltage, V_{sb} .

$$V_{th} = V_{th0} + \gamma \left(\sqrt{|2V_{fp}| + V_{sb}} - \sqrt{|2V_{fp}|} \right) \quad (2-5)$$

Where: V_{th0} Threshold Voltage when the source to body voltage is zero (V)

V_{fp} Flatband Voltage (V)

$$V_s = V_g + V_{th0} + \gamma \left(\sqrt{|2V_{fp}| + V_s - V_b} - \sqrt{|2V_{fp}|} \right) + \sqrt{\frac{2L_{M7,M8}I_{M7,M8}}{\mu_p C_{ox} W_{M7,M8}}} \quad (2-6)$$

The input-output transfer function of a source-follower with its body not tied to its source will be nonlinear and it is shown in Equation 2-6. A DC sweep simulation, as seen in Figure 2.7, is run to illustrate this nonlinearity. The PMOS transistor on the left has its body connected to the source resulting in zero V_{SB} . The PMOS transistor on the right has its body connect to VDD that leads to a non-zero V_{sb} . In this simulation, the VDD terminal is set to 5V and the VSS terminal is connected to ground. The vin signal is swept

from 5V to 0V. Figure 2.8 shows instantaneous slope of the source terminal for both of the PMOS transistor. The PMOS source-follower with its body tied to its source has a more constant slope than when its body is not tied to its source. Therefore, it is required to have the body of a source-follower tied to its source for a linear input-output transfer function. The AMI C5 process used in the experimental results is not a twin-well process and it is not possible to connect the body of an NMOS transistor to its source. Therefore, a PMOS source-follower is used instead of a NMOS although a PMOS transistor has a mobility that is half of a NMOS transistor.

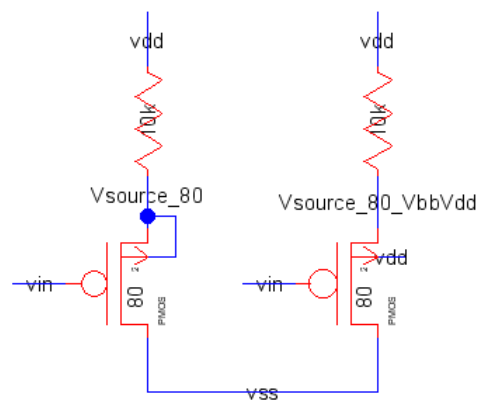


Figure 2.7 A simulation schematic used to compare body-effect in PMOS source-followers.

Transistors M1, M3 and M2, M4 with capacitor C_{LEFT} and C_{RIGHT} in Figure 2.3 serve the purpose as a forming switched-capacitor resistor in the DSM ADC. Node phi1B and phi2B are connected to the inverted signals of a 2-phase non-overlapping clock. Its frequency is equal to the master clock, f_{clk} . Figure 2.9 shows the waveform of the 2-phase non-overlapping clock signals, phi1, phi2, phi1B, and phi2B. Capacitor C_{LEFT} and C_{RIGHT}

are poly1-poly2 overlapped capacitors. The resistance of a switch capacitor resistor can be derived, as seen below, and finally shown in Equation 2-7.

$$I_{C_{LEFT},RIGHT} = C_{LEFT,RIGHT} \frac{\Delta V_{C_{LEFT},RIGHT}}{\Delta T} \quad (2-4)$$

$$I_{C_{LEFT},RIGHT} = C_{LEFT,RIGHT} \Delta V_{C_{LEFT},RIGHT} f_{clk} \quad (2-5)$$

$$\frac{\Delta V_{C_{LEFT},RIGHT}}{I_{C_{LEFT},RIGHT}} = \frac{1}{C_{LEFT,RIGHT} f_{clk}} \quad (2-6)$$

$$R_{switc hCap} = \frac{1}{C_{LEFT,RIGHT} f_{clk}} \quad (2-7)$$

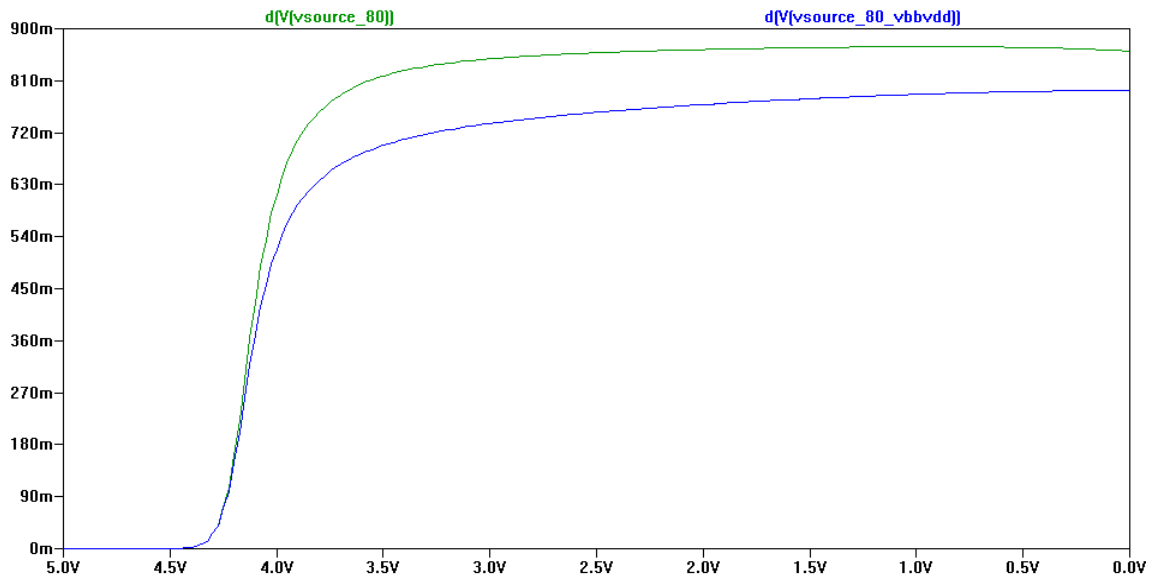


Figure 2.8 The differentiated output source voltage signal used to compare body-effect in PMOS source-followers.

During the first half of the clock period (when phi1B is low and phi2B is high), capacitor C_{LEFT} and C_{RIGHT} is charged up to V_{DD} . On the next half of the clock period

(when phi1B is high and phi2B is low), some of the charge stored on C_{RIGHT} will flow to VSS. The amount of current flow from capacitor C_{RIGHT} to VSS can be determined using Equation 2-3 and Equation 2-7. Since we know that the initial voltage on C_{RIGHT} is V_{DD} and the final voltage on C_{RIGHT} is $V_{RESET} + V_{th,M8}$, the magnitude of the reset current, I_{RESET} that flows is shown in Equation 2-10.

$$I_{RESET} = \frac{\Delta V_{C_{RIGHT}}}{RC_{RIGHT}} \quad (2-8)$$

$$I_{RESET} = \frac{V_{initial,C_{RIGHT}} - V_{final,C_{RIGHT}}}{RC_{RIGHT}} = \frac{V_{DD} - (V_{RESET} + V_{th,M8})}{\frac{1}{C_{RIGHT} f_{clk}}} \quad (2-9)$$

$$I_{RESET} = C_{RIGHT} f_{clk} (V_{DD} - V_{RESET} - V_{th,M8}) \quad (2-10)$$

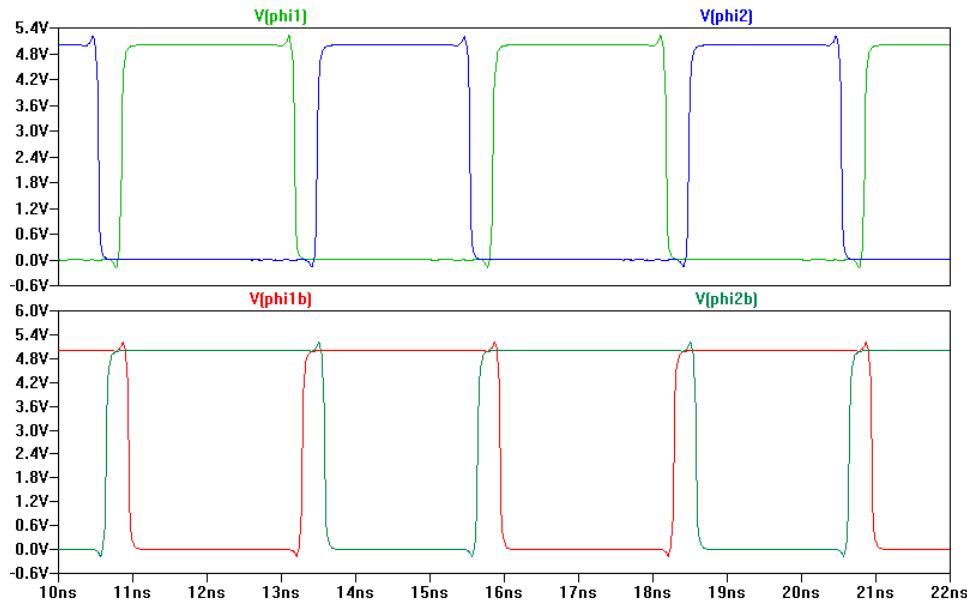


Figure 2.9 The waveform of a 2-phase non-overlapping clock.

The reset current, I_{RESET} will be mirrored over to the image branch through the current mirror transistors, M9 and M10. Assuming transistor M9 and M10 has identical threshold voltages and the drain voltages, the reset current, I_{RESET} , will be exactly equal to the mirrored reset current, $I_{RESET,mirror}$, as shown in Equation 2-11.

$$I_{RESET,mirror} = C_{RIGHT} f_{clk} (VDD - V_{RESET} - V_{th,M8}) \quad (2-11)$$

The right branch of the DSM, which is connected to the V_{RESET} input signal, serve the role as the float and valve in Figure 2.1. This unit controls the amount of charge removed from the sigma bucket. Capacitor C_{BUCKL} is serves the role as a “Sigma Bucket” in Figure 2.1 and it is also formed from poly1-poly2 overlapped.

During the first phase of the clock (phi1 is VDD and phi2 is VSS), the sense-amp (clocked comparator) turns transistor M5 off by taking the setting the negative terminal of the sense-amp to VDD . At the end of the first clock phase, the sense-amp senses the voltage difference between net_buckL and net_buckR and turns on M5 if the voltage on net_buckR is higher than net_buckL. The sense-amp will keep M5 off, if the voltage level on net_buckR is lower than net_buckL. An image current, I_{IMAGE} , will flow from C_{LEFT} into C_{BUCKL} if M5 is turned on. This current will raise the voltage on capacitor C_{BUCKL} . This image current serves the role of the “Delta Cup” as seen in Figure 2.1. This process will repeat N times over the entire conversion period. During this period, the sense-amp will turn on M5 for M times. The average image current, I_{IMAGE} , over N measurements can be derived using Equation 2-3 and Equation 2-7 and the final equation is shown in Equation 2-14.

$$I_{IMAGE} = \frac{M V_{C_{LEFT}}}{N R_{C_{LEFT}}} \quad (2-12)$$

$$I_{IMAGE} = \frac{M}{N} \left(\frac{V_{initial, C_{LEFT}} - V_{final, C_{LEFT}}}{R_{C_{LEFT}}} \right) = \frac{M}{N} \left(\frac{V_{DD} - (V_{IMAGE} + V_{th, M7})}{\frac{1}{C_{LEFT} f_{clk}}} \right) \quad (2-13)$$

$$I_{IMAGE} = \frac{M}{N} C_{LEFT} f_{clk} (V_{DD} - V_{IMAGE} - V_{th, M7}) \quad (2-14)$$

Over a long period of time, the current into and out of the sigma bucket, C_{BUCKL} is identical. Therefore, the image and reference current are equal to each other. Equation 2-17 shows the input-output transfer function that relates the analog input signal V_{IMAGE} and V_{RESET} to the digital code M over N measurements.

$$I_{IMAGE} = I_{RESET, mirror} \quad (2-15)$$

$$\frac{M}{N} C_{LEFT} f_{phi} (V_{DD} - V_{IMAGE} - V_{th, M7}) = C_{RIGHT} f_{phi} (V_{DD} - V_{RESET} - V_{th, M8}) \quad (2-16)$$

$$M = N \frac{C_{RIGHT}}{C_{LEFT}} \frac{(V_{DD} - V_{RESET} - V_{th, M8})}{(V_{DD} - V_{IMAGE} - V_{th, M7})} \quad (2-17)$$

The input-output transfer function for this CMOS DSM architecture is non-linear, which is undesirable in some situations (though in some situation, extremely bright or dark images may be desirable). To demonstrate this in more detail, let's assume N is 100, V_{DD} is 5V, V_{RESET} is 3V, both $V_{th, M7}$ and $V_{th, M8}$ is 1V, and C_{LEFT} and C_{RIGHT} are identical.

Figure 2.10 shows the input-output transfer function curve for this basic CMOS Imager DSM.

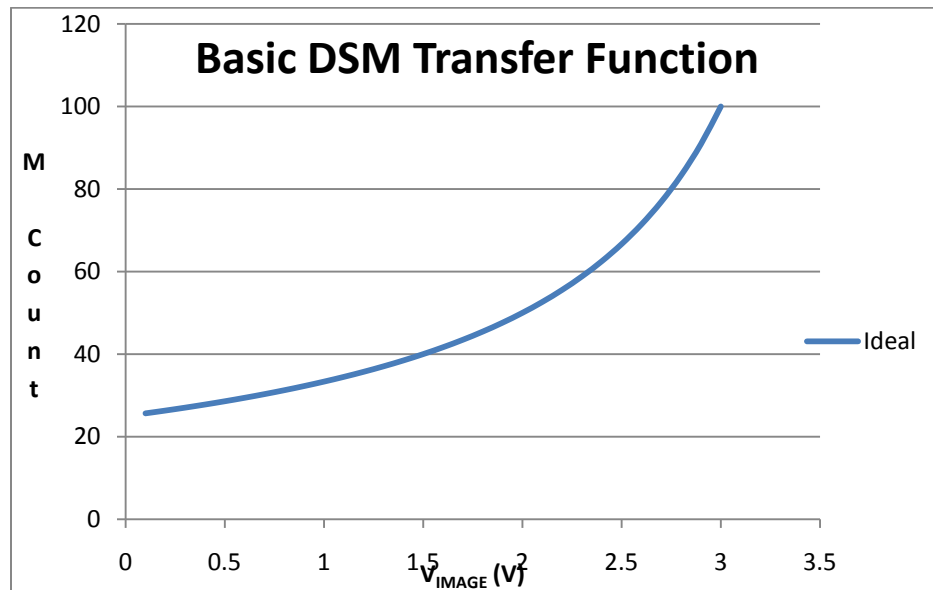


Figure 2.10 Basic CMOS Imager DSM Input-Output Transfer Function.

2.4 CMOS Image Sensor DSM with Reference Path

One of the biggest drawbacks in the DSM architecture discussed in Section 2.3 is that the input-output transfer function is non-linear. The input-output transfer function can be made linear by introducing a reference path to the basic CMOS Image Sensor DSM architecture [2]. Figure 2.11 shows the schematic of a DSM with reference path. Transistors M9, M10, M11, and M12 constitute the reference path.

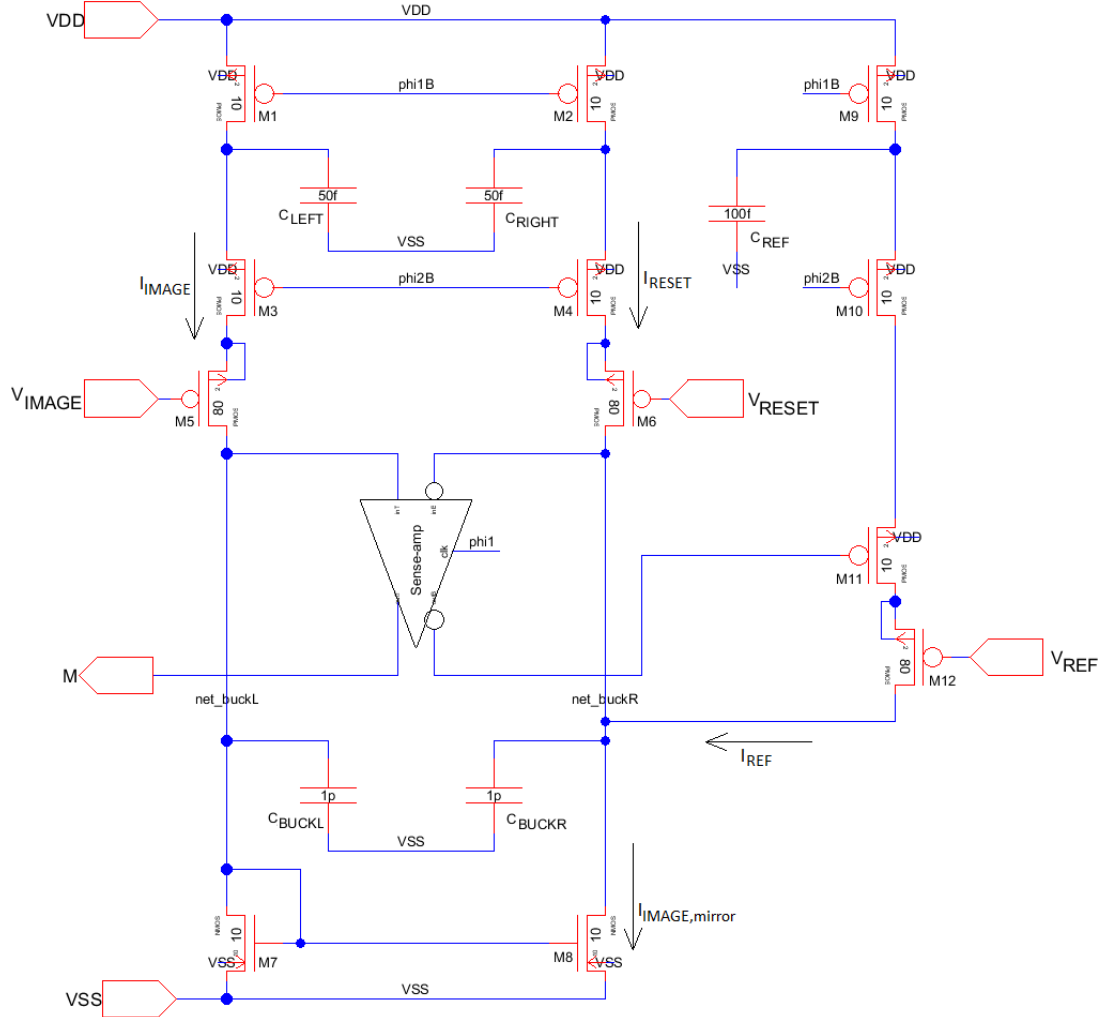


Figure 2.11 Schematic of a CMOS Imager Delta Sigma Modulator with reference path [2].

The magnitude of the reset current, I_{RESET} , in this architecture is similar to the reset current in the basic DSM, which is shown in Equation 2-10. However, the magnitude image current, I_{IMAGE} , in this architecture is different than the image current in the basic DSM. In this architecture, the image current flows into C_{BUCKL} at every clocked cycle, whereas in the basic DSM, the image current only flows into C_{BUCKL} when the

voltage on net_buckR is higher than net_buckL. The magnitude of the image current, I_{IMAGE} , for this DSM architecture is

$$I_{IMAGE} = C_{LEFT} f_{clk} (VDD - V_{IMAGE} - V_{th,M5}) \quad (2-18)$$

In this architecture, the output of the sense-amp is connected to transistor M11 instead. For the entire time of the first clock phase, the sense-amp turns off M11. At the end of the first clock phase, the sense-amp measures the voltage level on net_buckL and net_buckR and turns on M11 if the voltage level on net_buckL is higher than net_buckR. M11 remains off if the voltage level on net_buckL is lower than net_buckR. This process repeats for N times over the entire conversion period. During this period, M11 turns on for M amount of times and the average I_{VREF} current that flows is given by

$$I_{REF} = \frac{M}{N} \frac{\Delta V_{C_{REF}}}{R_{C_{REF}}} \quad (2-19)$$

$$I_{REF} = \frac{M}{N} \left(\frac{V_{initial,C_{REF}} - V_{final,C_{REF}}}{R_{C_{REF}}} \right) = \frac{M}{N} \left(\frac{VDD - (V_{REF} + V_{th,M12})}{\frac{1}{C_{REF} f_{clk}}} \right) \quad (2-20)$$

$$I_{REF} = \frac{M}{N} C_{REF} f_{clk} (VDD - V_{REF} - V_{th,M12}) \quad (2-21)$$

The DSM discussed in Section 2.3 mirrors the I_{RESET} current from the right branch to the left branch of the DSM. For this DSM, the I_{IMAGE} is mirrored from the left branch to the right branch of the DSM instead. The mirrored image current, $I_{IMAGE,mirror}$, is equivalent to the image current, I_{IMAGE} , if the drain voltage on M7 and M8 is identical.

$$I_{IMAGE,mirror} = I_{IMAGE} \quad (2-22)$$

$$I_{IMAGE,mirror} = C_{LEFT} f_{clk} (VDD - V_I - V_{th,M5}) \quad (2-23)$$

For this DSM, C_{BUCKR} is the sigma bucket. Over N clocked cycles, the sum of current into and out of the sigma bucket is identical. Equation 2-26 shows the input-output transfer function for this reference path DSM architecture. This equation relates the analog input signal, V_{IMAGE} and V_{RESET} , and the reference signal, V_{REF} , to the digital code M over N measurements.

$$I_{IMAGE} = I_{RESET} + I_{REF} \quad (2-24)$$

$$C_{LEFT} f_{clk} (VDD - V_{IMAGE} - V_{th,M5}) = C_{RIGHT} f_{clk} (VDD - V_{RESET} - V_{th,M6}) + \frac{M}{N} C_{REF} f_{clk} (VDD - V_{REF} - V_{th,M12}) \quad (2-25)$$

$$M = N \frac{(C_{LEFT} - C_{RIGHT}) VDD + (C_{RIGHT} V_{RESET} - C_{LEFT} V_{IMAGE}) + (C_{RIGHT} V_{th,M6} - C_{LEFT} V_{th,M5})}{C_{REF} (VDD - V_{REF} - V_{th,M12})} \quad (2-26)$$

$$M = N \frac{C_{LEFT,RIGHT} (V_{RESET} - V_{IMAGE} + V_{th,M6} - V_{th,M5})}{C_{REF} (VDD - V_{REF} - V_{th,M12})} \quad (2-27)$$

If the capacitance of C_{LEFT} and C_{RIGHT} are identical, Equation 2-26 can be simplified to Equation 2-27 and the input transfer function for this DSM architecture is linear. To demonstrate this in more detail, let's assume N is 100, VDD is 5V, V_{RESET} is

3V, V_{REF} is 1V, $V_{th,M5}$, $V_{th,M6}$, and $V_{th,M12}$ is also 1V, and $C_{LEFT,RIGHT}$ and C_{VREF} are identical. Figure 2.12 shows the input-output transfer function for this DSM.

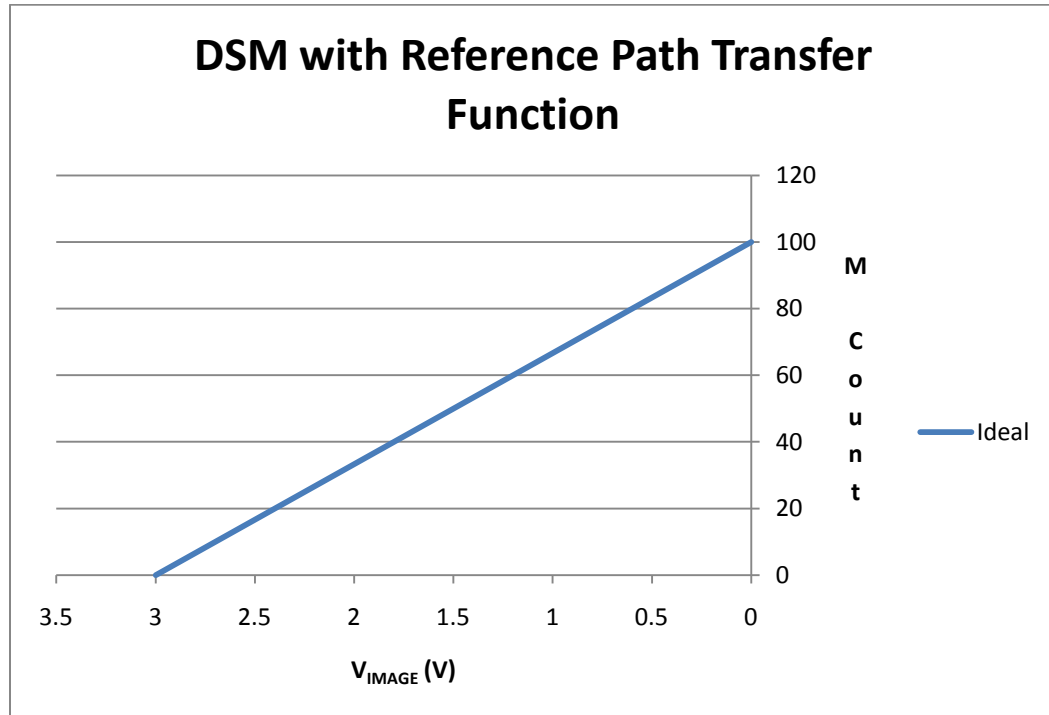


Figure 2.12 CMOS Imager DSM with Reference Path Input-Output Transfer Function.

Although this DSM has a linear transfer function, the transfer function is very susceptible to transistor threshold voltage mismatches. A fixed-pattern noise between the columns will occur if the threshold voltage on M5, M6, and M12 are not identical between all the DSMs in the array. A voltage-threshold mismatch on M5 and M6 will cause an offset error in the transfer function and a voltage-threshold mismatch on M12 will induce a gain error in the transfer function instead. An offset error will either shift

the transfer function upwards or downwards from ideal. On the other hand, a gain error will either increase or decrease the slope of the transfer function.

Figure 2.13 illustrates the behavior of the transfer function when threshold voltage mismatches on M5, M6, and M12 exist. The red line in Figure 2.13 is the transfer function of the DSM when a 0.25V threshold voltage delta between transistor M5 and M6 exist. The red line illustrates an offset error. On the other hand, the green line is the transfer function of the DSM when there is a 0.2V threshold mismatch on M12 and it illustrates a gain error.

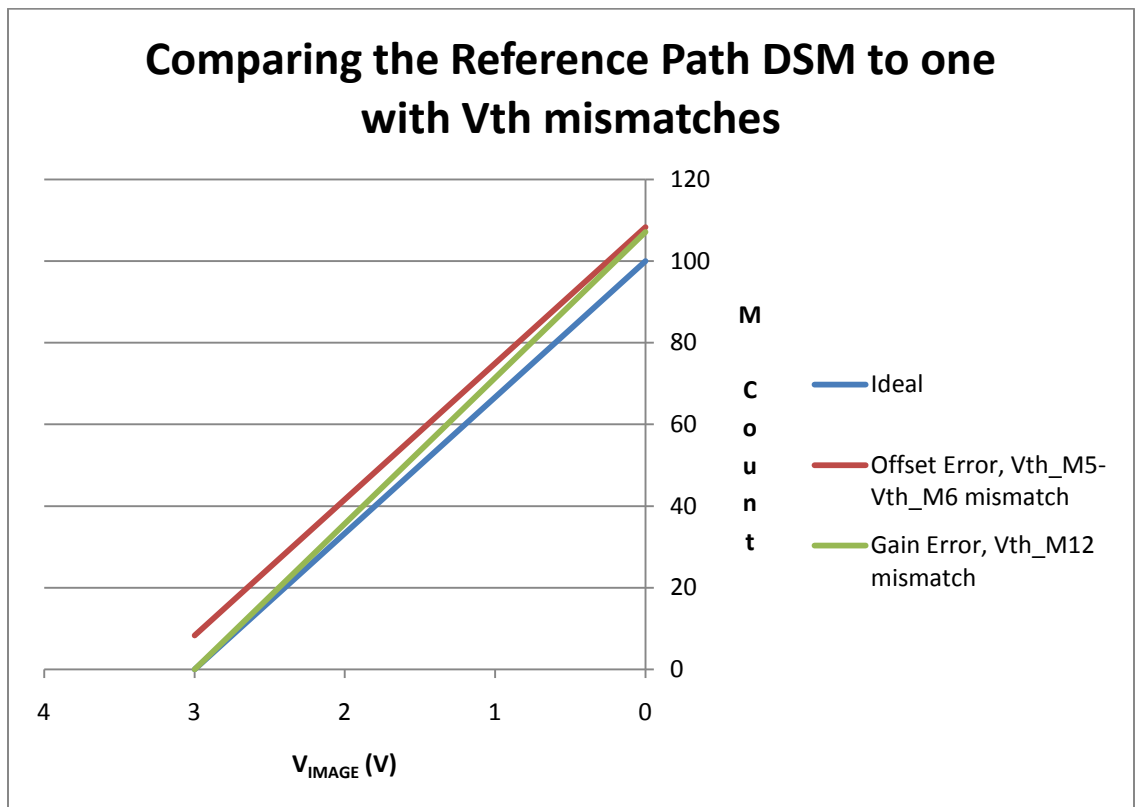


Figure 2.13 Comparing the ideal transfer function of a Reference Path CMOS Imager DSM to a transfer function with different threshold voltage mismatches.

2.5 CMOS Image Sensor DSM with Reference Path and Input Path Switching

As discussed in Section 2.4, an offset error will occur in the input-output transfer function if there is any voltage-threshold mismatch in the input transistors (M5 and M6 of Figure 2.11). A technique called *input path switching* can be used to eliminate offset error in the transfer function [1], [2]. The input path switching technique divides the whole conversion period into two equal halves ($N/2$ clock cycles). During the first half of the conversion period, the operation of the DSM does not differ from the sensing operation described in Section 2.4. However, on the second half of the conversion period, the DSM reverses its input terminals. The image input signal, V_{IMAGE} , and the reset input signal, V_{RESET} , switches gate connections. The digital output codes at the end of both halves of the sensing period are added together to get the final digital output code. This digital output code will be free from offset error.

Figure 2.14 shows the CMOS imager DSM with both reference path and input path switching improvements. For the first half of the sensing period, the path select control signals, SLT and SLB, are set to VDD and VSS respectively. This configuration connects the image input signal, V_{INPUT} , to the gate of M5 through M1S and the reset input signal, V_{RESET} , is connected to the gate of M6 through M3S. With this, the left branch current, $I_{LEFT,t=1}$, and right branch current, $I_{RIGHT,t=1}$, for the first half of sensing period are given by

$$I_{LEFT,t=1} = C_{LEFT} f_{clk} (VDD - V_{IMAGE} - V_{th,M5}) \quad (2-28)$$

$$I_{RIGHT,t=1} = C_{RIGHT} f_{clk} (VDD - V_{RESET} - V_{th,M6}) \quad (2-29)$$

In addition, the reference path is connected to the right branch of the DSM through M14S.

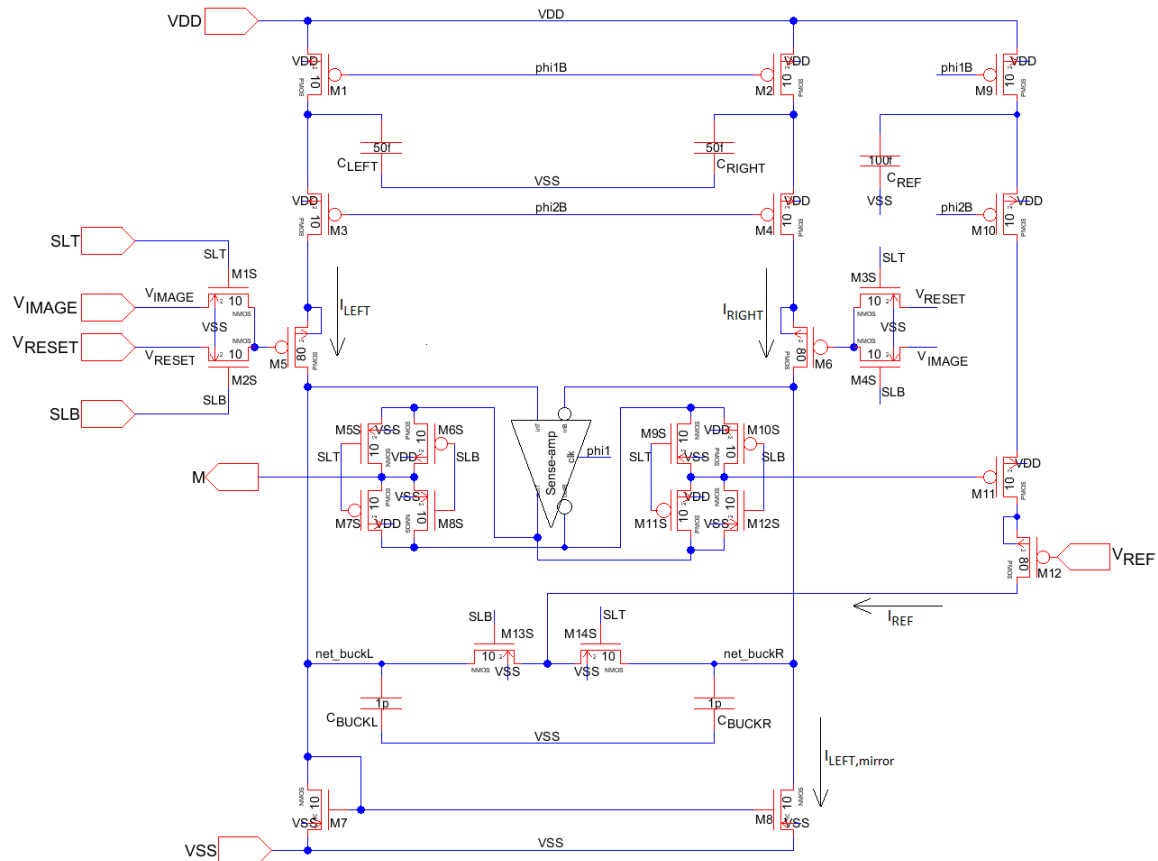


Figure 2.14 Schematic of a CMOS Imager Delta Sigma Modulator with reference path and input path switching [1].

For the entire conversion period, the positive and negative input terminals of the sense-amp are connected to net_buckR and net_buckL respectively. M5S, M6S, M7S, and M8S form a 2-bit analog multiplexer that steers either the negative or positive output of the sense-amp to the output terminal of the DSM, M. For this half of the conversion period, the positive terminal of the sense-amp is connected to the output of the DSM.

Another 2-bit analog multiplexer (M9S, M10S, M11S, and M12S) is needed to control which output terminal of the sense-amp is connected to the gate of M11. The negative terminal of the sense-amp is connected to the gate of M11 during the first half of the conversion period.

Just like before, the sense-amp turns on M11 if the voltage level on net_buckL is higher than net_buckR and leaves M11 off if the voltage level on net_buckL is lower than net_buckR. M11 will be turned on $M_{t=1}$ times for the first half of the conversion period and the average reference current, $I_{REF,t=1}$, that flows during this period is given by

$$I_{REF,t=1} = \frac{M_{t=1}}{N} \frac{V_{C_{REF}}}{R_{C_{REF}}} \quad (2-30)$$

$$I_{REF,t=1} = 2 \frac{M_{t=1}}{N} \left(\frac{V_{initial,C_{REF}} - V_{final,C_{REF}}}{R_{C_{REF}}} \right) = 2 \frac{M_{t=1}}{N} \left(\frac{V_{DD} - (V_{REF} + V_{th,M12})}{\frac{1}{C_{REF} f_{clk}}} \right) \quad (2-31)$$

$$I_{REF,t=1} = 2 \frac{M_{t=1}}{N} C_{REF} f_{clk} (V_{DD} - V_{REF} - V_{th,M12}) \quad (2-32)$$

$I_{LEFT,t=1}$ flow through the drain of M7 and it is mirrored over to the drain of M8. Over $N/2$ clock cycles, the sum of currents into C_{BUCKR} is zero. Therefore, the digital code representation, $M_{t=1}$, of the analog input signals, V_{IMAGE} and V_{RESET} , during the first half of the sensing period is determined using the following

$$I_{LEFT,mirror,t=1} = I_{LEFT,t=1} \quad (2-33)$$

$$I_{RIGHT,t=1} + I_{REF,t=1} = I_{LEFT,t=1} \quad (2-34)$$

$$\begin{aligned}
& C_{RIGHT} f_{clk} (VDD - V_{RESET} - V_{th,M6}) + 2 \frac{M_{t=1}}{N} C_{REF} f_{clk} (VDD - V_{REF} - V_{th,M12}) \\
& = C_{LEFT} f_{clk} (VDD - V_{IMAGE} - V_{th,M5})
\end{aligned} \tag{2-35}$$

$$M_{t=1} = \frac{N}{2} \left(\frac{C_{LEFT} (VDD - V_{IMAGE} - V_{th,M5}) - C_{RIGHT} (VDD - V_{RESET} - V_{th,M6})}{C_{REF} (VDD - V_{REF} - V_{th,M12})} \right) \tag{2-36}$$

Moving on to the second half of the sensing period, the path control signals, SLT and SLB, are set to VSS and VDD respectively. This will connect V_{IMAGE} to the gate of M8 through M2S and V_{RESET} is connected to the gate of M7 through M4S instead. The left branch current, $I_{LEFT,t=2}$, and right branch current, $I_{RIGHT,t=2}$, for the second half of sensing period are given by

$$I_{LEFT,t=2} = C_{LEFT} f_{clk} (VDD - V_{RESET} - V_{th,M5}) \tag{2-37}$$

$$I_{RIGHT,t=2} = C_{RIGHT} f_{clk} (VDD - V_{IMAGE} - V_{th,M6}) \tag{2-38}$$

The reference path is connected to the left branch of the DSM through M13S.

For the second half of the sensing period, the output of the DSM and the gate of M11 are connected to the negative and positive terminal of the sense-amp instead.

Whenever the voltage level on net_buckL is lower than net_buckR, the sense-amp turns on M11 and it is turned on for $M_{t=2}$ times. The average reference current, $I_{REF,t=2}$, that flows during this period is

$$I_{REF,t=2} = 2 \frac{M_{t=2}}{N} C_{REF} f_{clk} (VDD - V_{REF} - V_{th,M12}) \tag{2-39}$$

For this period of the sensing cycle, both the left branch current, $I_{LEFT,t=2}$, and the reference current, $I_{REF,t=2}$, flow through the drain of M7 and is mirrored over to the drain of M8. Just like the first half of the sensing period, the sum of current into C_{BUCKR} is zero. The digital code representation, $M_{t=2}$, of the analog input signal, V_{IMAGE} and V_{RESET} during the second half of the sensing period is

$$I_{LEFT,mirror,t=2} = I_{LEFT,t=2} + I_{REF,t=2} \quad (2-40)$$

$$I_{RIGHT,t=2} = I_{LEFT,t=2} + I_{VREF,t=2} \quad (2-41)$$

$$\begin{aligned} C_{RIGHT} f_{clk} (VDD - V_{IMAGE} - V_{th,M6}) &= C_{LEFT} f_{clk} (VDD - V_{RESET} - V_{th,M5}) \\ + 2 \frac{M_{t=2}}{N} C_{REF} f_{clk} (VDD - V_{REF} - V_{th,M12}) & \end{aligned} \quad (2-42)$$

$$M_{t=2} = \frac{N}{2} \left(\frac{C_{RIGHT} (VDD - V_{IMAGE} - V_{th,M6}) - C_{LEFT} (VDD - V_{RESET} - V_{th,M5})}{C_{REF} (VDD - V_{REF} - V_{th,M12})} \right) \quad (2-43)$$

If the output digital code representation of the analog input signal for both periods, $M_{t=1}$ and $M_{t=2}$, are added together, the final digital code representation of the analog input signal, M , is shown in Equation 2-45.

$$\begin{aligned} M = M_{t=1} + M_{t=2} &= \frac{N}{2} \left(\frac{C_{LEFT} (VDD - V_{IMAGE} - V_{th,M5}) - C_{RIGHT} (VDD - V_{RESET} - V_{th,M6})}{C_{REF} (VDD - V_{REF} - V_{th,M12})} \right) + \\ & \frac{N}{2} \left(\frac{C_{RIGHT} (VDD - V_{IMAGE} - V_{th,M6}) - C_{LEFT} (VDD - V_{RESET} - V_{th,M5})}{C_{REF} (VDD - V_{REF} - V_{th,M12})} \right) \end{aligned} \quad (2-44)$$

$$M = \frac{N}{2} \left(\frac{(C_{LEFT} + C_{RIGHT}) (V_{RESET} - V_{IMAGE})}{C_{REF} (VDD - V_{REF} - V_{th,M12})} \right) \quad (2-45)$$

The nominator of the input-output transfer function does not contain the voltage-threshold of M5 and M6. Hence, this DSM is immune to any offset error generated from the voltage-threshold mismatch of M5 and M6. However, a gain error still exists because the voltage-threshold from M12 is not removed from the denominator of the transfer function.

2.6 CMOS Image Sensor DSM with Reference Path, Input Path Switching, and Gain Error Correction

The gain error in the input-output transfer function can be eliminated by using 2 input reference voltage, V_{REF1} and V_{REF2} , instead. Figure 2-15 shows a DSM with the ability to cancel gain error cause by voltage-threshold mismatch on M12. A 4-phase non-overlapping clock generator is needed for this DSM and the schematic diagram is shown at Figure 2-16. Signal phi1, phi2, phi3, and phi4 are the four non-overlapping clock phases. The complement of these signals are phi1B, phi2B, phi3B, and phi4B. The frequency for each clock phase is 1/4th the rate of the master clock, f_{clk} .

The reference signal voltages needs to be on the gate on M12 a phase earlier and stays unchanged for the whole duration of the subsequent phase. This is to prevent any error in the magnitude of the two reference current, I_{REF1} and I_{REF2} . Hence, signal phi1 and phi3 are used to set the two reference voltages, V_{REF1} and V_{REF2} , on the gate of M12 instead of phi2 and phi4. A dummy capacitor is also added to the gate of M12 as a mean

to reduce the effects of charge injection and clock feed-through on the reference voltages stored on the gate of M12 when phi1 and phi3 signal transitions from high to low.

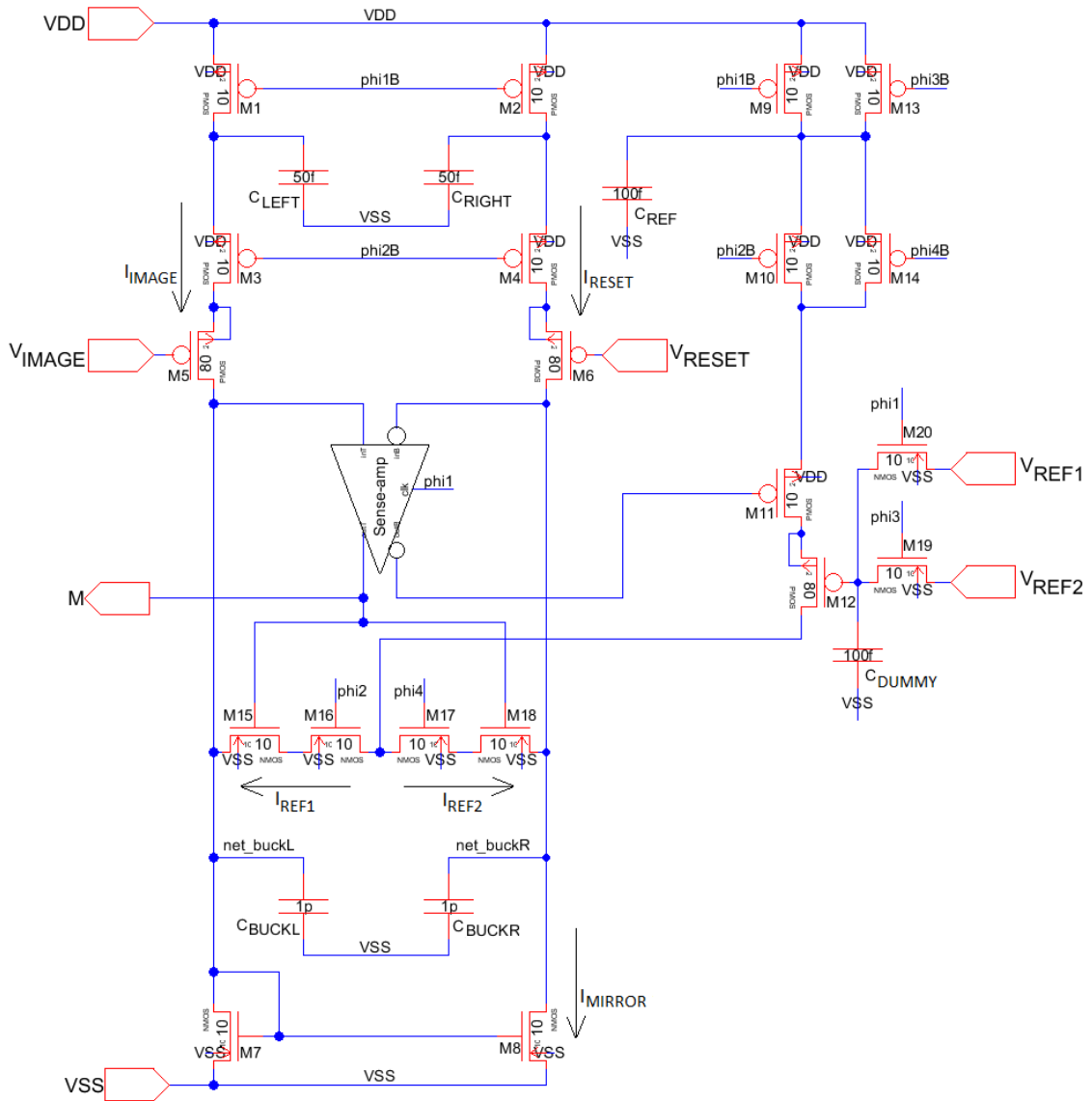


Figure 2.15 Schematic of a CMOS Imager Delta Sigma Modulator with gain error correction.

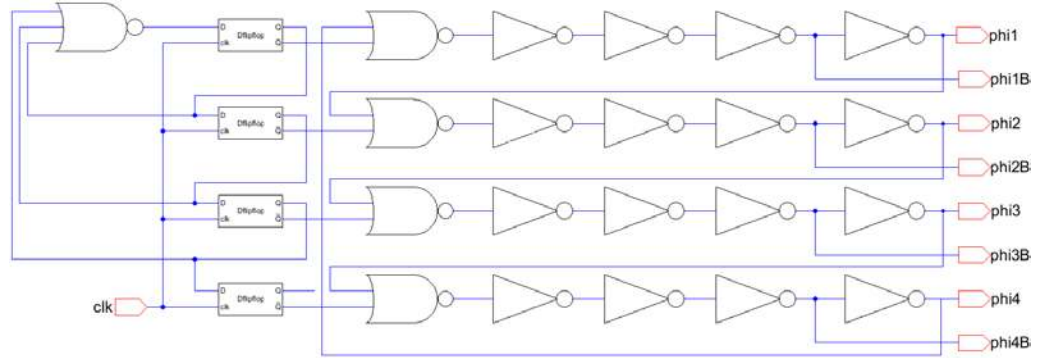


Figure 2.16 Schematic diagram of a 4-phase non-overlapping clock generator.

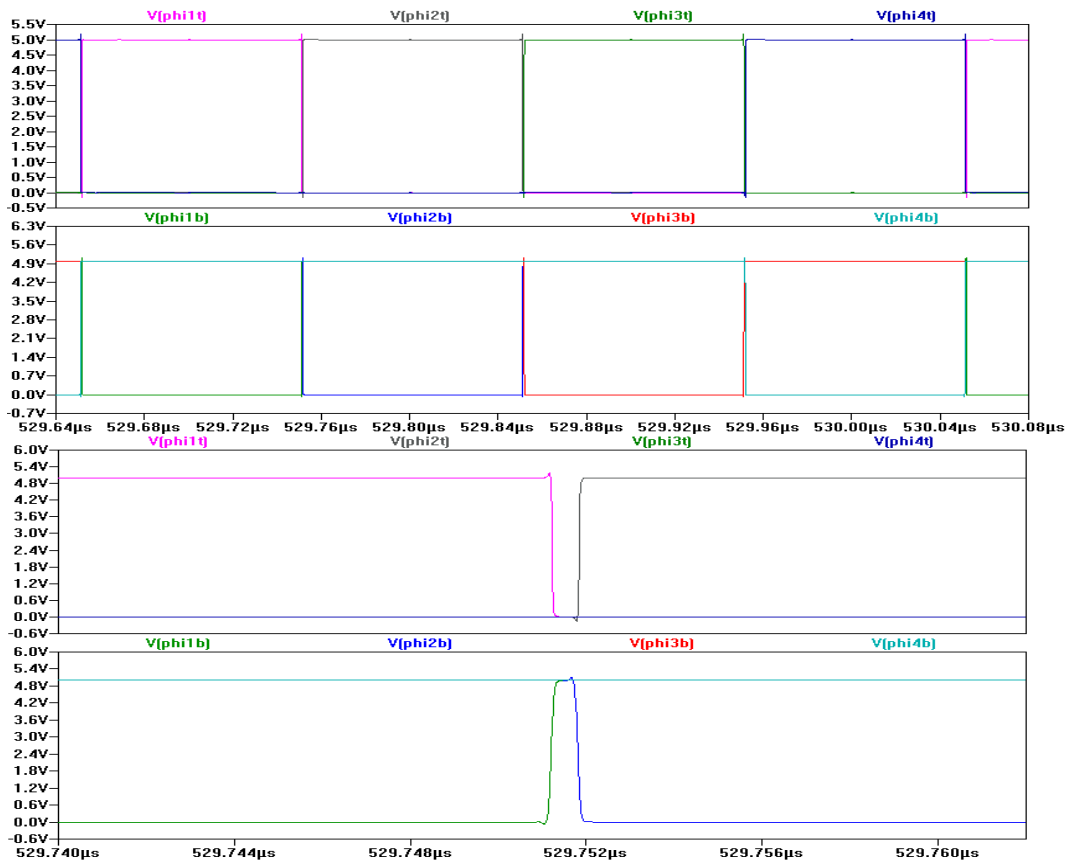


Figure 2.17 The waveform of a 4-phase non-overlapping clock signal. The bottom figure shows the close-up view when transitioning from the first phase to the second phase.

The sense-amp in this DSM also measures the voltages on capacitor C_{BUCKL} and C_{BUCKR} at the end of the first phase of the clock but it turns on M11, M15, and M18 instead for the remaining three clock phases if the voltage on capacitor C_{BUCKL} is lower than the voltage on capacitor C_{BUCKR} . M11, M15, and M18 will be left off for the remaining three clock phases if the voltage on capacitor C_{BUCKL} is higher than the voltage on capacitor C_{BUCKR} . The sense-amp turns on M11, M15, and M18 for M times for the entire conversion period.

The gain error correction occurs during every clock period. The process begins on the first phase of the clock by turning on M10 which set the voltage level on C_{REF} to VDD . At the same time, M20 turns on and allows the first reference signal, V_{REF1} , to propagate to the gate of M14. Capacitor C_{LEFT} and C_{RIGHT} is also set to VDD by M1 and M2 during this clock phase.

On the next clock phase, M10 and M16 turns on and the first reference current, I_{REF1} will flow from C_{REF} to C_{BUCKL} if the sense-amp turns on M11, M15, and M18. The average reference current that flows into C_{BUCKL} is

$$I_{REF1} = \frac{M}{N} \frac{\Delta V_{C_{REF1}}}{R_{C_{REF1}}} \quad (2-46)$$

$$I_{REF1} = \frac{M}{N} \left(\frac{V_{initial, C_{REF1}} - V_{final, C_{REF1}}}{R_{C_{REF1}}} \right) = \frac{M}{N} \left(\frac{VDD - (V_{REF1} + V_{th, M12})}{\frac{4}{C_{REF} f_{clk}}} \right) \quad (2-47)$$

$$I_{REF1} = \frac{1}{4} \frac{M}{N} C_{REF} f_{clk} (VDD - V_{REF1} - V_{th, M12}) \quad (2-48)$$

Also during this phase, the image current, I_{IMAGE} , and reset current, I_{RESET} , will flow from C_{LEFT} and C_{RIGHT} to C_{BUCKL} and C_{BUCKR} respectively. The magnitude of I_{IMAGE} and I_{RESET} are

$$I_{IMAGE} = \frac{1}{4} C_{LEFT} f_{clk} (VDD - V_{IMAGE} - V_{th,M5}) \quad (2-49)$$

$$I_{RESET} = \frac{1}{4} C_{RIGHT} f_{clk} (VDD - V_{RESET} - V_{th,M8}) \quad (2-50)$$

On the third phase of the clock, the voltage on C_{REF} is force back to VDD by M13. At the same time, M19 turns on and the second reference voltage, V_{REF2} , is propagated to the gate of M12. If the sense-amp turns on M11, M15, and M18, the second reference current, I_{REF2} , will flow from C_{REF} to C_{BUCKR} on the fourth phase of the clock. Current I_{REF2} will only flow for M times over the entire conversion period and its average magnitude is

$$I_{REF2} = \frac{M}{N} \frac{\Delta V_{C_{REF2}}}{R_{C_{REF2}}} \quad (2-51)$$

$$I_{REF2} = \frac{M}{N} \left(\frac{V_{initial,C_{REF2}} - V_{final,C_{REF2}}}{R_{C_{REF2}}} \right) = \frac{M}{N} \left(\frac{VDD - (V_{REF2} + V_{th,M12})}{\frac{4}{C_{REF} f_{clk}}} \right) \quad (2-52)$$

$$I_{REF2} = \frac{1}{4} \frac{M}{N} C_{REF} f_{clk} (VDD - V_{REF2} - V_{th,M12}) \quad (2-53)$$

At every clock period, I_{IMAGE} and I_{REF1} will flow through the drain of M7 and the currents will be mirrored over to M8. Over N clock cycles, the sum of current into

C_{BUCKR} is ideally zero and the digital relationship between the analog inputs signals with respect to the reference signals is

$$I_{MIRROR} = I_{IMAGE} + I_{REF1} \quad (2-54)$$

$$I_{RESET} + I_{REF2} = I_{MIRROR} = I_{IMAGE} + I_{REF1} \quad (2-55)$$

$$\begin{aligned} & \frac{1}{4} C_{RIGHT} f_{clk} (VDD - V_{RESET} - V_{th,M8}) + \frac{1}{4} \frac{M}{N} C_{REF} f_{clk} (VDD - V_{REF2} - V_{th,M12}) \\ &= \frac{1}{4} C_{LEFT} f_{clk} (VDD - V_{IMAGE} - V_{th,M5}) + \frac{1}{4} \frac{M}{N} C_{REF} f_{clk} (VDD - V_{REF1} - V_{th,M12}) \end{aligned} \quad (2-56)$$

$$M = N \left(\frac{C_{LEFT} (VDD - V_{IMAGE} - V_{th,M5}) - C_{RIGHT} (VDD - V_{RESET} - V_{th,M8})}{C_{REF} (V_{REF1} - V_{REF2})} \right) \quad (2-57)$$

The transfer function for this DSM shows that it is robust to any gain error cause by voltage-threshold mismatch. This is because the denominator of the transfer function does not contain the voltage-threshold of any transistor in the DSM. The gain of the DSM is controlled by the two reference voltage signals, V_{REF1} and V_{REF2} . The difference between V_{REF1} and V_{REF2} determines the gain of the DSM.

However, this DSM is still prone to offset error as the nominator of the transfer function contains the voltage-threshold of M5 and M6. Path switching methodology can be applied to this DSM to reduce the effects of offset error. Figure 2.18 illustrates the DSM with reference path, input path switching and gain error correction.

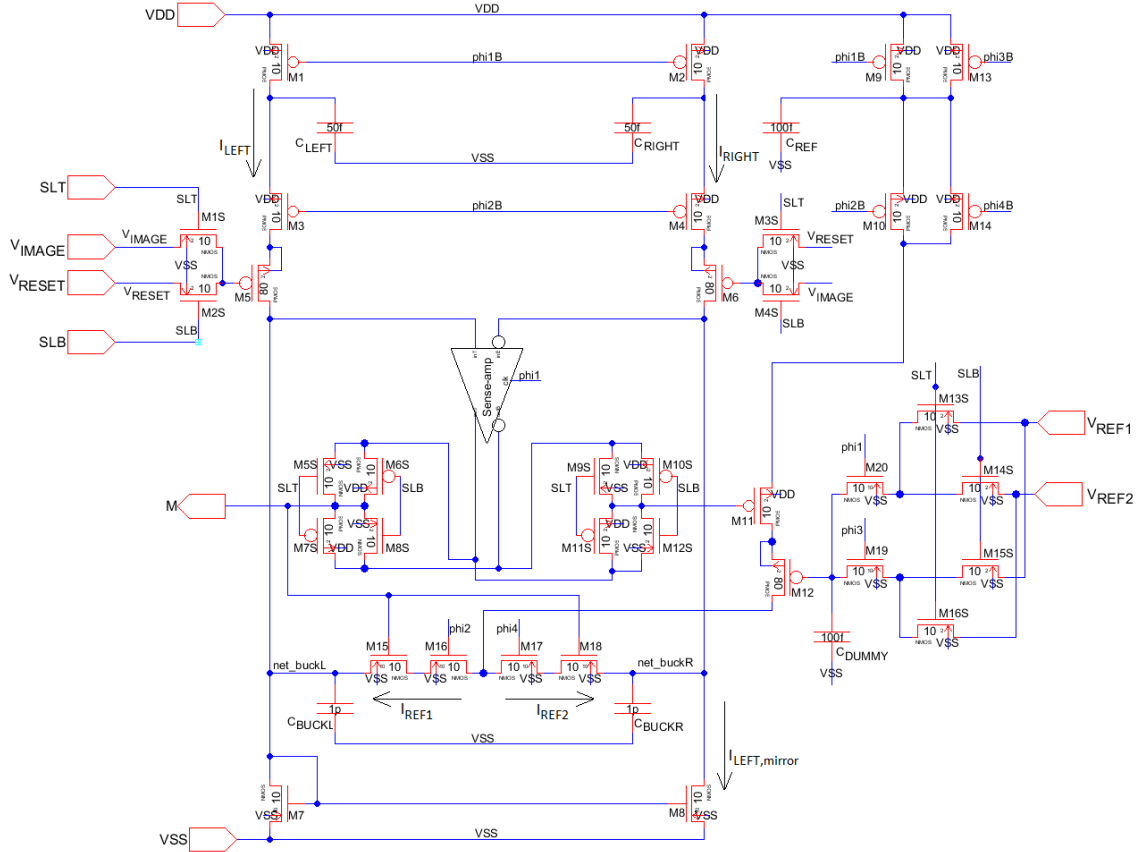


Figure 2.18 Schematic of a CMOS Imager Delta Sigma Modulator with reference path, input path switching and gain error correction.

Just like conversion method discussed in Chapter 2.5, conversion period is now divided into 2 equal halves where each half is $N/2$ clock cycles long. On the first half of the conversion period, the control signals SLT and SLB are set to VDD and VSS respectively. For this half of the conversion period, the digital code representation of the analog input signals with respect to the two reference input signals, $M_{t=1}$, is

$$M_{t=1} = \frac{N}{2} \left(\frac{C_{LEFT} (VDD - V_{IMAGE} - V_{th,M5}) - C_{RIGHT} (VDD - V_{RESET} - V_{th,M6})}{C_{REF} (V_{REF1} - V_{REF2})} \right) \quad (2-58)$$

On last half of the conversion period, the control signals SLT and SLB are now set to V_{SS} and V_{DD} respectively. The digital code representation of the analog input signals with respect to the two reference input signals for the last half of the sensing period, $M_{t=2}$, is

$$M_{t=2} = \frac{N}{2} \left(\frac{C_{LEFT} (V_{DD} - V_{IMAGE} - V_{th,M6}) - C_{RIGHT} (V_{DD} - V_{RESET} - V_{th,M5})}{C_{REF} (V_{REF1} - V_{REF2})} \right) \quad (2-59)$$

Similarly, the digital code representation from the 2 halves are added together at the end of the conversion period to receive the final digital output code of the DSM with both gain and offset correction. Its final digital output code is

$$M = M_{t=1} + M_{t=2} = \frac{N}{2} \left(\frac{(C_{LEFT} + C_{RIGHT})}{C_{REF}} \frac{(V_R - V_I)}{(V_{REF1} - V_{REF2})} \right) \quad (2-60)$$

The input-output transfer function for this DSM does not include the voltage-threshold of any transistor in the DSM. This means that the DSM is robust to any offset or gain error cause by voltage-threshold mismatches. However, a gain error might still occur if the capacitor ratio between the sum of C_{LEFT} and C_{RIGHT} and C_{REF} is not identical between the many DSMs in the array.

The least significant bit voltage, V_{LSB} , for this DSM is specified in Equation 2-61 seen below. The bit accuracy of the conversion increases linearly with the number of clock cycles, N , during the conversion period.

$$V_{LSB} = \frac{2}{N} \left(\frac{C_{REF}}{(C_{LEFT} + C_{RIGHT})} \right) (V_{REF1} - V_{REF2}) \quad (2-61)$$

In addition, the input dynamic range is given by Equation 2-62. The input dynamic range can be accurately controlled by the reference voltage signals, V_{REF1} and V_{REF2} . In low light environment, the dynamic range of the input signals is reduced. If a gain stage is not used to amplify the input signals, the image decoded will be dark. This DSM can compensate for this reduction of the input dynamic range without using a gain stage. This is can be accomplished by reducing the delta between V_{REF1} and V_{REF2} . On the other hand in a bright light environment, the DSM can compensate for the increase in input dynamic range by increasing the delta between V_{REF1} and V_{REF2} .

$$ADC \text{ input range} = \left(\frac{C_{LEFT} + C_{RIGHT}}{C_{REF}} \right) \frac{1}{(V_{REF1} - V_{REF2})} \quad (2-62)$$

CHAPTER 3: SIMULATION RESULTS AND TEST CHIP INFORMATION

3.1 Simulation Results

A voltage source is added in series with the gate of a transistor to simulate a variation in its threshold voltage. For all the simulations ran in this chapter, N is 512, V_{DD} is 5V, V_{SS} is 0V, V_{REF1} is 3.5V, V_{REF2} is 2.25V, V_R is 3.5V and V_I is decrease from 3.5V to 1V. This will yield a input dynamic range of 2.5V. The frequency of the master clock is 10 MHz.

Figure 3.1 shows the simulation result for the DSM with just the reference path, like in Figure 2.11. This DSM is prone to offset and gain error if voltage-threshold mismatch exists between the many DSMs in the array.

The red line in Figure 3.1 is the transfer function of the DSM when a negative 0.25V voltage offset is applied to the gate of M5. The transfer function of the DSM shift upwards from ideal and this is known as offset error. If a positive voltage offset is applied to the gate of M5, the transfer function will move downwards from ideal instead. On the other hand, the green line is the transfer function of the DSM when a negative 0.2V offset is applied to the gate of M12 and this is gain error. A negative voltage offset will reduce the slope of the transfer function and a positive voltage offset will increase the slope.

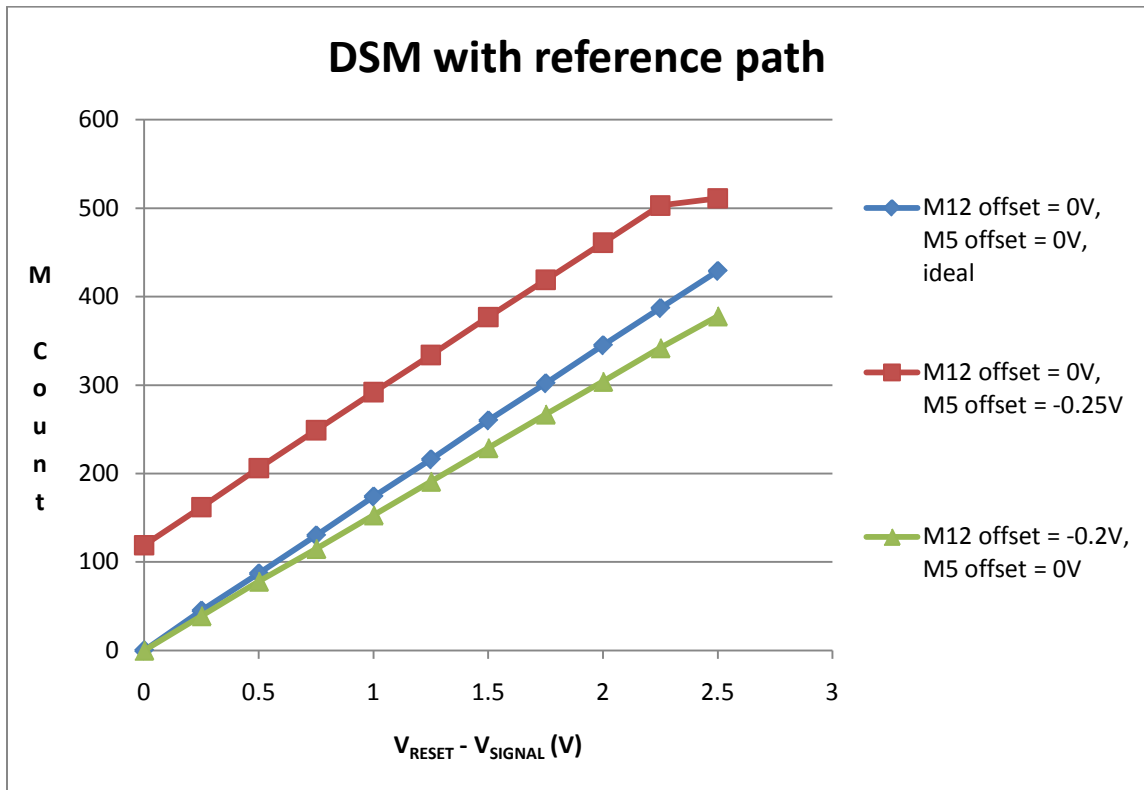


Figure 3.1 Simulation Results for the CMOS Imager DSM with reference path.

Different voltage offsets were applied to the gate of M12 and M5 to simulate offset and gain error.

The DSM with reference path and gain error correction like in Figure 2.15 should be robust to gain error cause by voltage-threshold mismatch. Figure 3.2 shows simulation results of the DSM with reference path and gain error correction. A negative or positive 0.2V voltage offset on M12 does not reduce or increase the slope of the transfer function. However, offset error still occurs if a voltage-threshold offset exists on M5, as shown as the purple line in Figure 3.2.

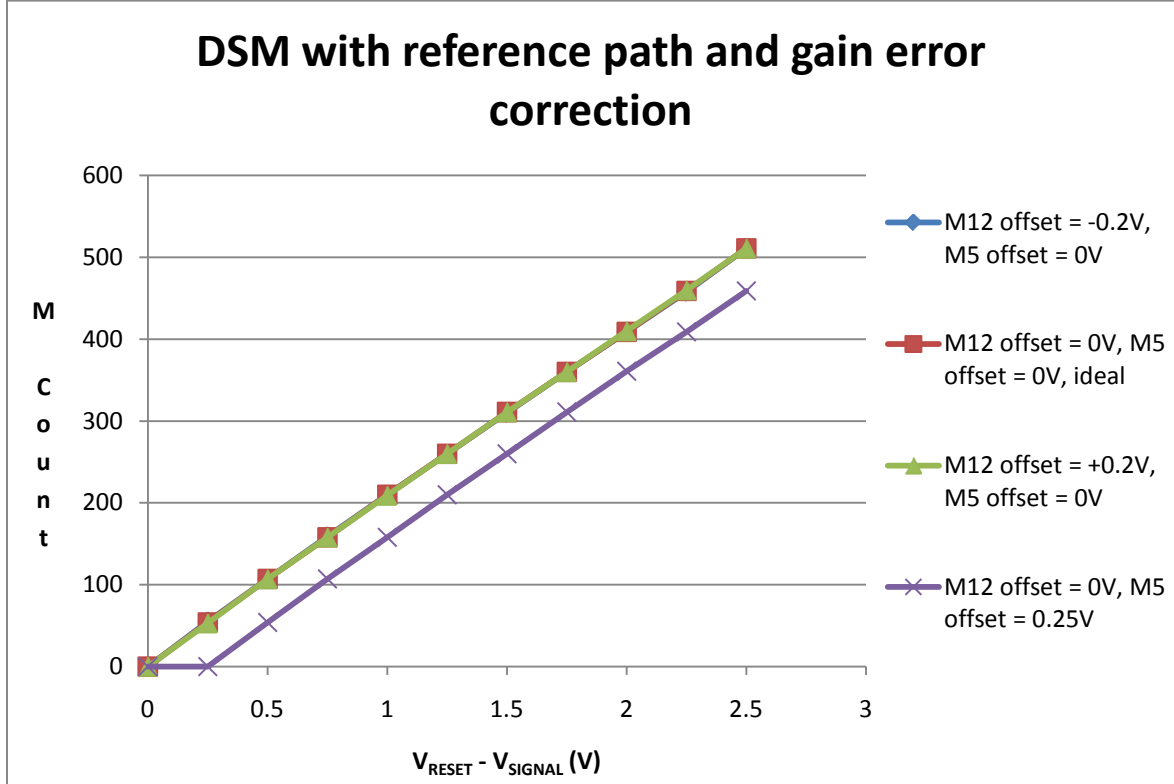


Figure 3.2 Simulation Results for the CMOS Imager DSM with reference path and gain error correction. Different voltage offsets were applied to the gate of M12 and M5 to simulate offset and gain error.

A DSM with reference path, input path switching, and gain error correction should be robust to both offset and gain error cause by voltage-threshold mismatch. Multiple simulations were run on the DSM in Figure 2.18 and its results are shown in Figure 3.3. A 0.25V voltage offset on M5 does not shift the transfer function downward and the transfer function tracks the ideal transfer function except on the front and tail end. The transfer function curves upward at the front end and curves downward at the tail end. This magnitude of the deviation from the ideal line is equivalent to the digital code representation of the offset value, 0.25V. This means any input signal that falls on either

curve will produce an erroneous digital code representation. Therefore, the input dynamic range of the DSM is reduced by twice the voltage-threshold offset on M5. A DSM with voltage offsets on both M5 and M12 will have a similar transfer function as the DSM with voltage offsets on only M5, as shown in Figure 3.4.

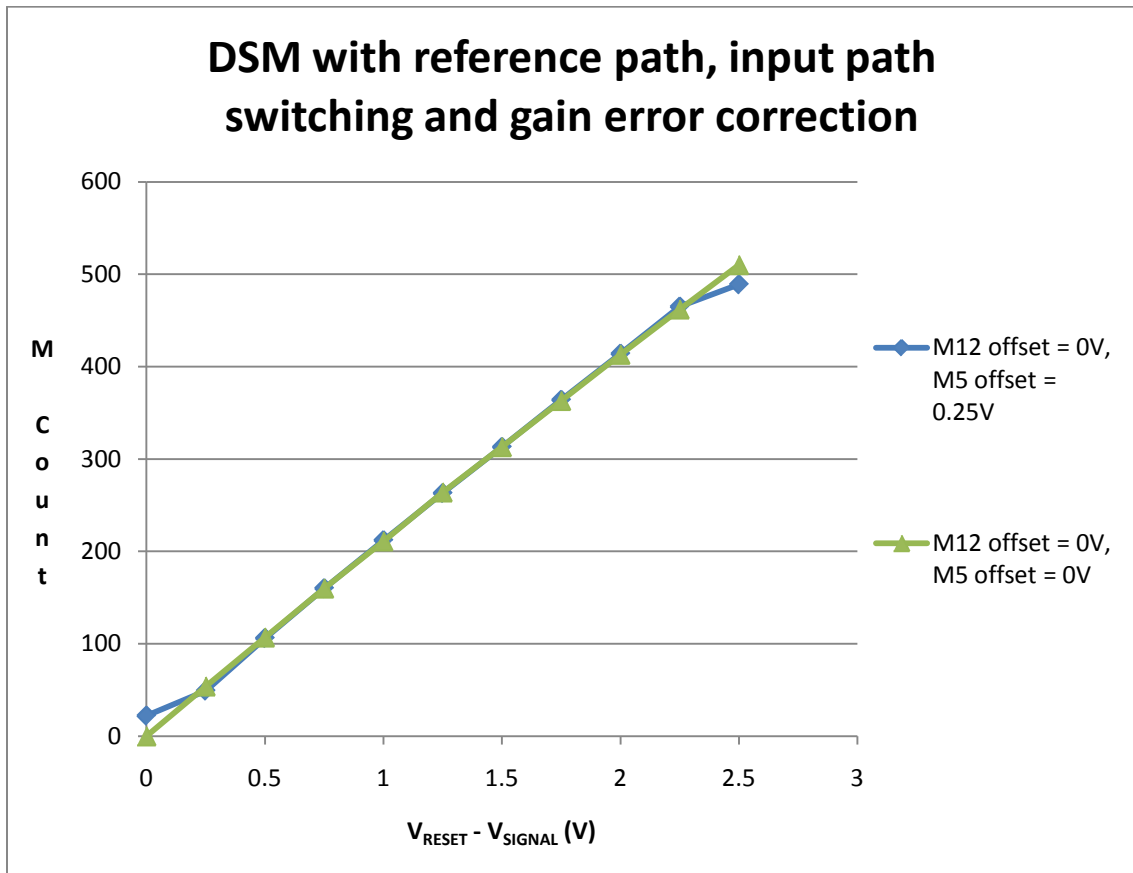


Figure 3.3 Simulation Results for the CMOS Imager DSM with reference path, input path switching, and gain error correction. A 0.25V voltage offsets was applied to the gate of M5 to simulate offset error.

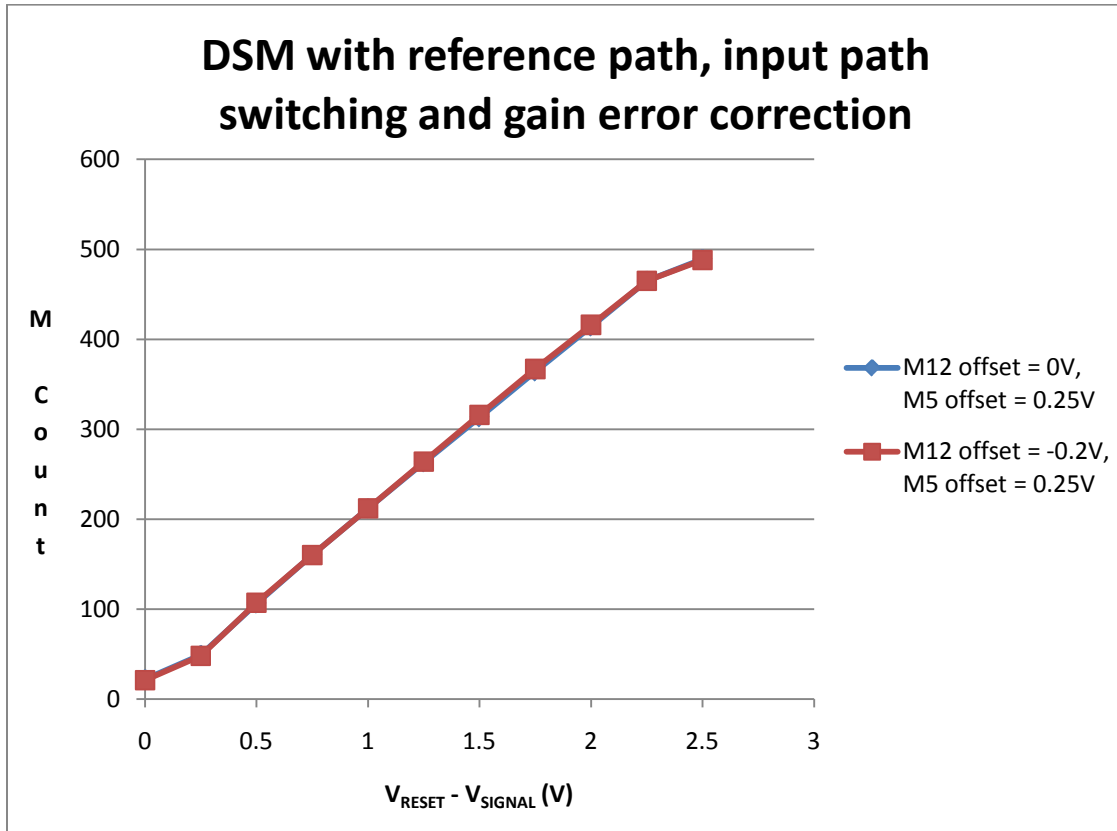


Figure 3.4 Simulation Results for the CMOS Imager DSM with reference path, input path switching, and gain error correction. Different voltages offsets were applied to M5 and M12 to simulate offset and gain error.

3.2 Layout

The test chip consists of the DSM in Figure 2.11, 2.14, 2.15, and 2.18 . The standalone sense-amp and 4 phase non-overlapping clock generator (Figure 2.16) were also included in the layout for direct testing.

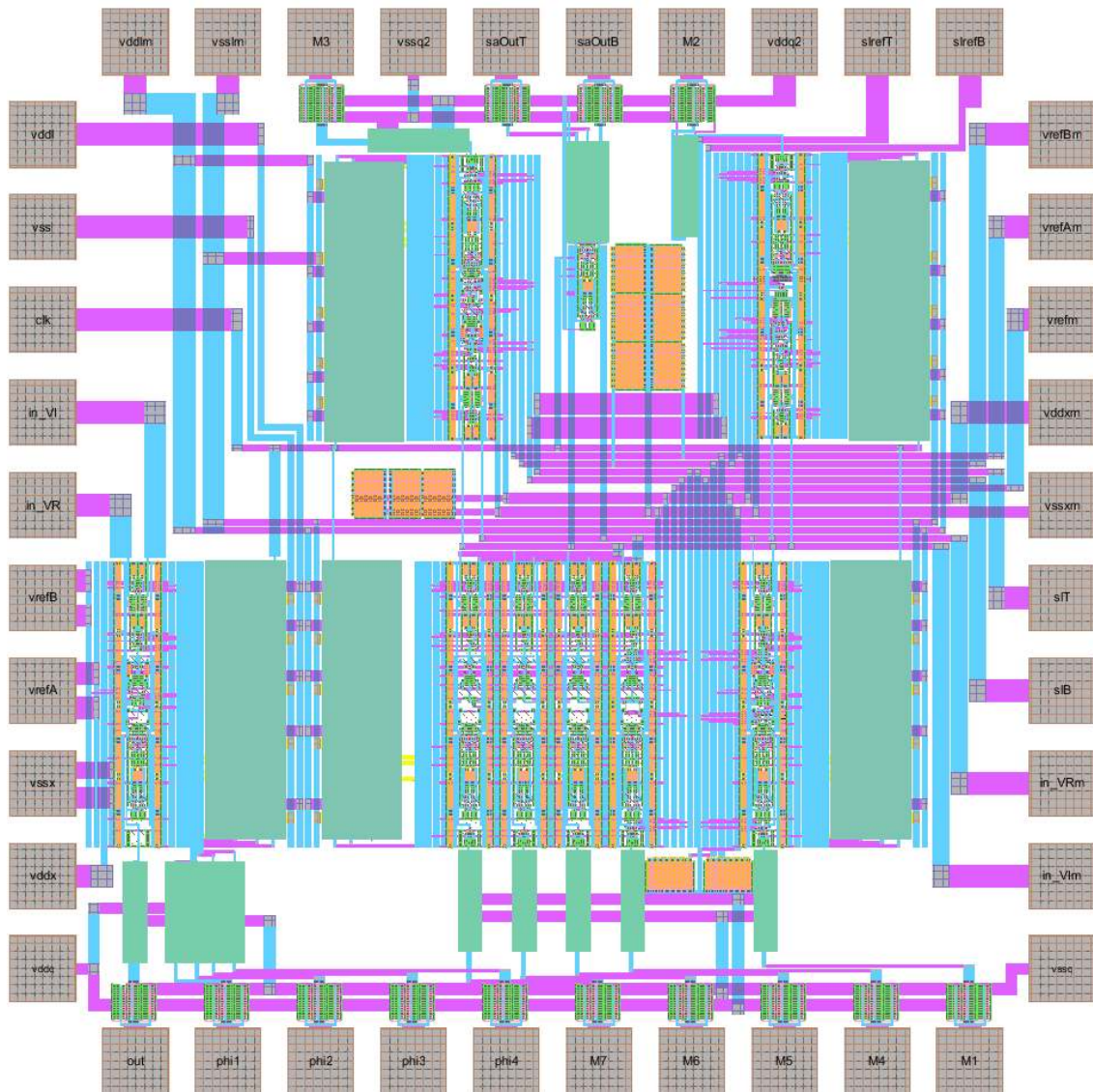
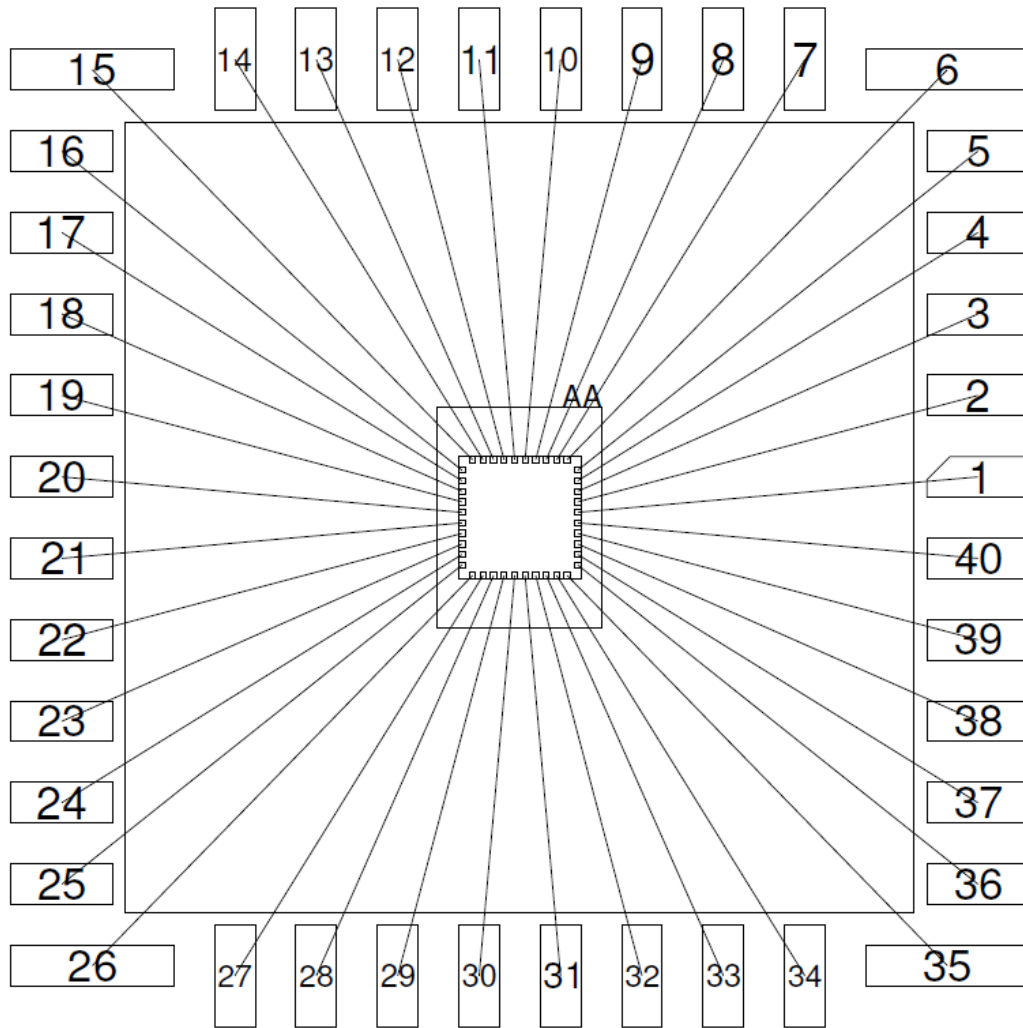


Figure 3.5 Test chip full layout

3.3 General Test Chip Information



Qty: 5		V01W-AA		DIP40	
		(83050)			
40 wires; longest is 5436; shortest is 4010 um					
Minimum pad size: 60 x 60; minimum pad pitch: 105 um					
	Design_name: TOP_DSM_NEW				
	Customer Account: 2831				
	Die Size: 1648 (+0 / -72) x 2201 (+0 / -72) um				
	Die Rotation in Cavity: None				
	Cavity Size: 7874 um x 7874 um				
				11-FEB-2010 17:29:11	

Figure 3.6 Bonding diagram for test chip provided by MOSIS.

Table 3.5 Pin Description

Pin Number	Pin Type	Pin Description
1,12,14,17,23,36	Supply	VSS Supply. There are separate VSS signals for the multiple DSM ADCs, sense-amp, 4-phase nonoverlapping clock generator, and output drivers.
2,8,15,16,24,25	Supply	VDD Supply. There are separate VDD signals for the multiple DSM ADCs, sense-amp, 4-phase nonoverlapping clock generator, and output drivers.
3,4,5,21,22	Input	The different DSM ADCs input reference signals.
6,7,39,40	Input	The path control signals for the DSM ADCs.
19,37	Input	The input image signals for the DSM ADCs.
20,38	Input	The input reset signals for the DSM ADCs.
18	Input	The clock input signal for the multiple DSMs, sense-amp, and 4-phase nonoverlapping clock generator
27,28,29,30	Output	The output of the 4 phase non-overlapping clock generator
10,11	Output	The output of the sense-amp
9,13,26,31,32,33,34,35	Output	The output of the multiple DSM ADCs

CHAPTER 4: CONCLUSION AND FUTURE WORK

4.1 Conclusion

A CMOS image sensor using a per-column DSM ADC has many advantageous over a pipeline ADC. However, transistor voltage-threshold mismatches between the many DSMs in the array causes offset and gain error in its transfer. These errors will lead to fixed-pattern noise. A complex digital signal processor is needed if correction is to be done in the digital domain. A DSM ADC with offset error correction was introduced by Montierth to help reduce some of this error. To remove both gain and offset error cause by transistor voltage-threshold mismatch, a new DSM ADC architecture was proposed in this thesis.

The bit accuracy of a pipeline ADC is fixed by design and cannot be increased without a complete redesign. The DSM ADC bit accuracy is proportional to the number of clock cycles during the sensing period. A minimum of 1024 clock cycles is needed if a 10-bit conversion accuracy is required. On the other hand, a conversion period of 4096 clock cycles is required for a 12-bit conversion accuracy. Increasing the bit accuracy on a DSM ADC is easy and does not require a major redesign.

A pipeline ADC will require a separate gain stage to increase or reduce the input dynamic range. This extra gain stage requires additional power and layout area. The per-column DSM ADC is able to reduce or increase the input dynamic range by simply

controlling the delta between the two reference signals, V_{REF1} and V_{REF2} . A large delta between the two reference signals indicates a large input dynamic range and vice versa.

4.2 Future Work

As noted previously, the conversion period of the DSM ADC is proportional to the conversion bit accuracy. A very long conversion period may not be desirable. The charge stored on the sample and hold capacitors will leak over time and conversion errors may appear if the voltage on the sample and hold capacitor deviates from its original sampled voltages. Therefore, introducing a topology to increase the sampling rate of the DSM may be a topic for future work. One method may be to introduce a parallel K-path sampling of the DSM. The DSM with parallel K-path sampling will sample the voltage on net_buckL and net_buckR for K extra times at every clock period. The length of the entire conversion period is N/K clock cycles instead.

The DSM ADC proposed in this thesis only removes offset and gain error caused by transistor voltage-threshold mismatches. However, if a capacitor ratio mismatch occurs between the sum of C_{LEFT} and C_{RIGHT} and C_{REF} , a gain error might still occur. A topology to reduce the effect of gain error from capacitance ratio mismatch may also be another topic for future work.

REFERENCES

- [1] Dennis Glen Montierth, *Using Delta-Sigma Modulation for Sensing in a CMOS Imager*, thesis (M.Sc), Boise State University, 2008

- [2] Baker, R. Jacob, *CMOS Circuit Design, Layout and Simulation*, 2nd Edition, IEEE press, 2005, ISBN 0-471-70055-X

- [3] Eric R. Fossum, “CMOS Image Sensors: Electronic Camera-On-A-Chip”, IEEE Transactions on Electron Devices, Vol. 44, No. 10, pp. 1689-1698, October 1997.

- [4] Noble, P.J.W, “Self-scanned silicon image detector arrays”, IEEE Transactions, Vol. 15, No. 4, pp. 202-209, April 1968.

- [5] D. James, L. Klibanov, G. Tompkins, St. J. Dixon-Warren, *Inside CMOS Imager Sensor Technology*, Retrieved June 1, 2009, from www.chipworks.com.tw/resources/whitepapers/Inside-CMOS.pdf.

- [6] John Coghill, DALSA Corp, 2003, *Digital Imaging Technology 101*, Retrieved May 31, 2009, from <https://classes.yale.edu/04-05/enas627b/lectures/EENG427107DigitalImaging.pdf>